Available online at www.sciencedirect.com
ScienceDirect
Physics of Life Reviews 8 (2011) 169–199
PHYSICS of LIFE reviews
www.elsevier.com/locate/plrev

Review

Modeling the impact of global warming on vector-borne infections

Eduardo Massad [a,b,*], Francisco Antonio Bezerra Coutinho [a], Luis Fernandez Lopez [a], Daniel Rodrigues da Silva [a]

[a] *School of Medicine, University of São Paulo and LIM01-HCFMUSP, SP, Brazil*
[b] *London School of Hygiene and Tropical Medicine, United Kingdom*

Received 27 September 2010; received in revised form 3 January 2011; accepted 3 January 2011

Available online 14 January 2011

Communicated by J. Fontanari

Abstract

Global warming will certainly affect the abundance and distribution of disease vectors. The effect of global warming, however, depends on the complex interaction between the human host population and the causative infectious agent. In this work we review some mathematical models that were proposed to study the impact of the increase in ambient temperature on the spread and gravity of some insect-transmitted diseases.

Keywords: Global warming; Vectors; Infections; Modeling

1. Introduction

Disagreement still remains about the extent to which recent warming in global temperatures deviates from normal climatic cycles [1]. In other words, the role of anthropogenic sources in the unequivocal warming of the Earth observed in the last decades is to be determined yet. However, few deny the fact that the global temperature has increased since around 1900 [2]. During this century, Earth's average surface temperature rises are likely to exceed the safe threshold of 2 °C above preindustrial average temperature [3]. Also undeniable is the fact that human activities are causing a net annual addition of 3 Gt of carbon to the atmosphere [4]. Among climatologists, in particular, there is now a general agreement that the main influence on the world's climate in the near future will be the warming effect of anthropogenic greenhouse gases [2].

Climate change due to greenhouse warming is not just an environmental issue but also a health issue [3] and it would have both direct and indirect effects upon human health [5,6]. The direct effects, via temperature change, thermal extremes and increased natural disasters, are easier to predict than are the various indirect and delayed effects [4]. Approximately 22,000 to 45,000 heat-related deaths occurred across Europe over two days in August 2003 [7,8], probably the hottest summer in Europe in over 500 years, with average temperatures 3.5 °C above normal [9]. Direct effects of climate change on human health ranges from cardiovascular mortality and respiratory illness due to heat-

* Corresponding author at: Av. Dr. Arnaldo 455, São Paulo, CEP 01246-903, SP, Brazil.
E-mail address: edmassad@usp.br (E. Massad).

1571-0645/$ – see front matter
doi:10.1016/j.plrev.2011.01.001

waves, to malnutrition from crop failures [10]. However, it is likely that the indirect effects, in particular the alteration in patterns of vector-borne infections, will outweigh the direct effects.

The increase in temperature will affect the spread and transmission rates of vector-borne infections. Temperature affects rate of pathogen maturation and replication within mosquitoes, the density of insects in a particular area, and increases the likelihood of infection [3]. Vector reproduction, parasite development cycle, and bite frequency generally rise with temperature; therefore malaria, tick-borne encephalitis, and dengue fever will become increasingly widespread.

Of particular concern is the expected shift in the 16 °C isotherm, which indicates the limit for reproduction and maintenance of anopheline mosquitoes, vectors of malaria [11]. The threat posed by malaria is especially worrisome. The disease is increasingly resistant to antimalarial drugs and is spreading out of control over large areas of South America and Asia. In addition to the new environmental conditions for the thriving of malaria vectors, the optimum temperature for the deadly *Plasmodium falciparum* parasite is 26 °C, which may soon be common in southern Europe and the United States. This may cause tremendous devastation because the emergence of *falciparum* malaria in an area where people have no natural immunity may lead to death rates as high as 50% [12].

The distribution of insects transmitting malaria, as well as other tropical infections, and their seasonal abundance are determined by the favorable temperature conditions and the presence of breeding places, which depend to a great extent on precipitation. With the increase in the average global temperature it is necessary to develop techniques to foresee and prevent outbreaks [11].

One of the first attempts at entomological forecasting was that of Gill [13], who in 1921 defined the areas where malarial epidemics are possible. On the basis of the temperature and humidity factors limiting the distribution of mosquitoes and necessary for the development of malaria parasite, Gill determined the areas where malarial transmission would be unlikely. Today, modern techniques for temperature and humidity measurement, such as remote sensing of meteorological data for the study of the distribution and abundance of vectors of disease [14], are widening the possibilities of entomological forecasting. The precise calculations, however, should be performed upon entomological knowledge that would correlate the factors determining the abundance and distribution of vectors and their life cycle [11].

Global warming will certainly affect the abundance and distribution of disease vectors [15]. The effect of global warming, however, depends on the complex interaction between the human host population and the causative infectious agent.

Some models suggest that vector-borne diseases will become more common as the Earth warms, although caution is needed in interpreting these predictions. Clearly, global warming will cause changes in the epidemiology of infectious diseases.

It should be mentioned that an increase in temperature might displace the current geographic distribution of those diseases and although transmission might get established in new areas, it might also disappear from current areas of transmission making predictions about the net balance in transmission rather uncertain [11].

For a comprehensive review on the impacts of global change on vector-borne diseases see [16].

2. Theoretical basis of vector-borne infections [17]

The central parameter related to the intensity of transmission of infections is the so-called basic reproduction number R_0 [17], defined by Macdonald [18] as the number of secondary infections produced by a single infective in an entirely susceptible population. Originally applied in the context of malaria, R_0 is a function of the vector population density as related to the host population, m, the average daily biting rate of the vector, a, the host susceptibility, b, the mosquito's susceptibility, c, the vector mortality rate, μ, the parasite extrinsic incubation period in days, n, and the parasitemia recovery rate, r, according to the (now) historical equation:

$$R_0 = \frac{ma^2bc\exp[-\mu n]}{r\mu} \tag{1}$$

(actually, Macdonald denoted R_0 as z_0 in his original paper). From the definition of the basic reproduction number it can be demonstrated that if R_0 is not greater than one, that is, when an index case (the first infective individual) is not able to generate at least one new infection, the disease dies out. Hence, in the original Macdonald analysis, R_0 coincides with the threshold for the infection persistence. For an interesting historical account of R_0, see [19].

3. The classical Macdonald analysis

In his 1952 seminal paper, Macdonald [18] addressed the problem of a system involving one vector (*Anopheles* mosquitoes) and one host (men). As mentioned above, his definition of R_0 is the number of secondary infections in the first generation, that is, produced by a single infectee along its entire infectiousness period. We shall deduce an explicit expression for R_0 from an intuitive perspective to show that it coincides with the threshold for the establishment of the disease. We do this because, as shown in the next section, for more complex systems this approach does not work in such a simple way.

Let us begin by assuming that the index case is a human host. The question to be answered is how many human secondary infections this index case produces in his/her entire infectiousness period.

Let N_m be the number of female mosquitoes. Let a be the average daily biting rate female anophelines inflict in the human population. The number of bites in the human population per units of time is, therefore, $N_m a$. Let N_h be the number of humans and r be the rate of recovery from parasitemia in the human cases. Therefore, the index case produces $\frac{N_m a}{N_h r} c_{h\to m}$ infected mosquitoes, where $c_{h\to m}$ is the probability that a mosquito gets the infection after biting an infective human. Those $\frac{N_m a}{N_h r} c_{h\to m}$ infected mosquitoes, in turn, produce $a \frac{N_m a}{N_h r} c_{h\to m} \frac{1}{\mu} b_{m\to h} e^{-\mu\delta}$ new human cases in the first generation, where $\frac{1}{\mu}$ is the average life expectance of mosquitoes, $b_{m\to h}$ is the probability that a human gets the infection after being bitten by an infective mosquito and $e^{-\mu\delta}$ is the fraction of the infected mosquito population that survives through the extrinsic incubation period δ of the parasite. Note that, once infective a mosquito is assumed to remain so for life. Therefore, the expression for R_0 is [18]:

$$R_0 = a \frac{N_m a}{N_h r} c_{h\to m} \frac{1}{\mu} b_{m\to h} e^{-\mu\delta} \tag{2}$$

Similarly, if we begin with an infective mosquito as an index case, and compute the number of infected mosquitoes this index case produces in the first generation we get the same expression.

Let us now see how this deduction can be performed by a dynamical system approach.

Let Y_h be the number of infected humans, and Y_v the number of infected vectors. We can write

$$\begin{aligned} \frac{dY_h}{dt} &= \frac{Y_v a}{N_h} b_{v\to h} S_h - r Y_h \\ \frac{dY_v}{dt} &= \frac{S_v(t-\delta) a}{N_h} c_{h\to m} e^{-\mu\delta} Y_h(t-\delta) - \mu Y_v \end{aligned} \tag{3}$$

where S_h and S_v are the number of susceptible humans and vectors, respectively.

To deduce the threshold for the disease to establish in the human population we analyze the stability of the trivial solution $S_h = N_h$, $S_v = N_v$, $Y_v = Y_h = 0$, that is, the solution representing the absence of the infection. Linearizing the system (3) around the trivial solution we get

$$\begin{aligned} \frac{dy_h}{dt} &= y_v a b_{v\to h} - r y_h \\ \frac{dy_v}{dt} &= \frac{N_v a}{N_h} c_{h\to m} e^{-\mu\delta} y_h(t-\delta) - \mu y_v \end{aligned} \tag{4}$$

where y_v and y_h are small deviations from zero. From the system (4), assuming solutions of the type $y_h = Ae^{\lambda t}$ and $y_v = Be^{\lambda t}$, we get the following characteristic equation for λ

$$\begin{vmatrix} -(\lambda + r) & a b_{v\to h} \\ \frac{N_v a}{N_h} c_{h\to m} e^{-\mu\delta} e^{-\lambda\delta} & -(\lambda + \mu) \end{vmatrix} = 0 \tag{5}$$

or

$$\lambda^2 + (\mu + r)\lambda + \mu r - \frac{N_v a}{N_h} c_{h\to m} e^{-\mu\delta} e^{-\lambda\delta} a b_{v\to h} = 0 \tag{6}$$

It follows that the roots of Eq. (5) or (6) have negative real parts if

$$\mu r - \frac{N_v a}{N_h} a b_{v\to h} c_{h\to m} e^{-\mu\delta} > 0 \tag{7}$$

The above result is the same as that obtained by the intuitive McDonald's approach.

This still holds true for slightly more complex systems, like those with one vector and two host populations or two vectors with one host population. In these cases, the expression for R_0 is partitioned in a sum with the individual terms of each component of the transmission chain [20].

4. The next generation operator

In a classical paper Diekmann et al. [21] propose a new definition of the basic reproduction number for infections which we now study how it compares with the classical Macdonald definition described above.

Those authors define R_0 as being the greatest eigenvalue of an operator which they call "the next generation operator (NGO)". The case of vector-transmitted infections was analyzed in a recent book by Diekmann and Heesterbeek [22].

In this section we give the next generation operator for the case of one-vector/one-host, exemplified by malaria. In this case, the next generation operator reduces to a two-by-two matrix

$$NGO = \begin{pmatrix} A_{v\to v} & A_{v\to h} \\ A_{h\to v} & A_{h\to h} \end{pmatrix} \tag{8}$$

The elements have the following interpretation. The element $A_{v\to h}$, for instance, means the number of infected humans generated by a single infected vector during its infectious period. Therefore, we have

$$\begin{aligned} A_{v\to v} &= 0 \\ A_{v\to h} &= a\frac{1}{\mu}b_{m\to h}e^{-\mu\delta} \\ A_{h\to h} &= 0 \\ A_{h\to v} &= \frac{N_m a}{N_h r}c_{h\to m} \end{aligned} \tag{9}$$

Essentially, the NGO is the mean infectious output over all possible progressions of the infection within the host individual and therefore contains any process that influences output of infectious material to others. In particular, the NGO was derived without appealing to the dynamical system (3).

In this case the greatest eigenvalue of the NGO matrix, that is, R_0^{NGO}, is

$$R_0^{NGO} = \sqrt{a\frac{N_m a}{N_h r}c_{h\to m}\frac{1}{\mu}b_{m\to h}e^{-\mu\delta}} \tag{10}$$

which is the square root of the Macdonald R_0. It follows from the general theory of the Next Generation Operator [19] that if $R_0^{NGO} < 1$ ($R_0^{NGO} > 1$) the disease cannot (can) invade the host population.

From Eq. (1) or (10) it is possible to estimate the critical density of female mosquitoes, m^*, below which the disease will naturally disappear:

$$m^* = \frac{r\mu}{a^2 bc\exp[-\mu n]} \tag{11}$$

Another interesting parameter proposed by Macdonald is the *Sporozoite rate* [18], S, which, like R_0 is not a rate but a number. This parameter is defined as the proportion of female mosquitoes with sporozoites in their salivary glands for the case of malaria, or simply the prevalence of infection in the mosquito population. It incorporates the equilibrium proportion of infected individuals in the host population, y, and has the form:

$$S = \frac{acy\exp[-\mu n]}{acy+\mu} \tag{12}$$

Some years later Garret-Jones [23] defined a derived parameter, which highlighted the entomological components of Macdonald's equation, the so-called *Vectorial Capacity*, C. This parameter describes the daily rate at which future inoculations arise from a currently infective case, and its formulation in the context of Eq. (1) is:

$$C = \frac{ma^2 \exp[-\mu n]}{\mu} \tag{13}$$

The per capita rate at which susceptibles acquire the infection is called *Force of Infection* [24], normally denoted h in the literature of vector-borne infections, and λ in the directly transmitted infections texts. It is the equivalent to the incidence density rate of the classical epidemiological texts. For vector-borne infections, the force of infection is the effective inoculation rate, that is, the number of infective bites per unit of time in a non-immune individual receives. It may take the form:

$$h = mabS \tag{14}$$

that is, those bites ma, inflicted by infected, S, and infective, b, females.

Alternatively, it is possible to estimate h from the vectorial capacity, as done by the Dietz–Molineaux–Thomas model in the Garki project [25]. Those authors proposed to estimate malarial force of infection as related to the vectorial capacity by:

$$h = b\big[1 - \exp(-Cy)\big] \tag{15}$$

which is based on the following interpretation. In a stable situation, where C and y are constants, each member of the population receives C potentially infective contacts per day; a fraction y of these contacts originates from infectives and represents inoculations; therefore, the average number of inoculations per person per day is Cy; assuming a Poisson distribution, the probability of receiving no inoculation is $\exp(-Cy)$ and the probability of receiving at least one inoculation is $1 - \exp(-Cy)$, of which a fraction b is effectively infective.

5. Effects of seasonality on vector-borne infections [26]

In subtropical regions vector-borne infections show a resurgent pattern with yearly epidemics, which start in the months characterized by heavy rains and heat (summer), peaking some three or four months after the beginning of the rainy season. In the dry months (winter) the number of cases drops essentially to zero due to the virtual disappearance of the vectors.

Before describing the model proposed to describe the effects of seasonality on vector-borne infections, however, we introduce the main assumptions related to the mosquito life cycle and the seasonality considered.

The mosquito goes through four separate and distinct stages of its life cycle: Egg, Larva, Pupa, and Adult. Each of these stages can be easily recognized by its special appearance. How long each stage lasts depends on both temperature and species characteristics. For instance, *Culex tarsalis*, a common California (USA) mosquito, might go through its life cycle in 14 days at 70 °F and take only 10 days at 80 °F. On the other hand, some species have naturally adapted to go through their entire life cycle in as little as four days or as long as one month [27].

In temperate and subtropical regions the aedes population density presents marked variations along the year, peaking in the summer and dropping to very low densities in the winter. Seasonal and climatic effects on mosquitoes influence transmission. Temperature and humidity affect mosquitos' longevity and activity, gonadotrophic cycle length, oviposition rates, eggs survival rates and eggs hatching rates. Also, as a water breeding species, mosquitoes require standing water to reproduce, thus cold winters and/or dry summers substantially reduce mosquitoes breeding and feeding [28].

Therefore, seasonality can be driven by the several biological and environmental mechanisms above. As described in the next section, we choose to model seasonality by forcing the rate at which eggs mature into adults to change periodically along the year. This assumption can be better understood by the fact that in northern univoltine mosquitoes species adults usually emerge in the spring and lay eggs, which do not hatch until next spring, diapausing along the winter [28, p. 89]. Of course, in tropical regions, diapausing of multivoltine species is less extreme and the rate of eggs hatching in the dry season significantly diminishes, but does not go to zero.

The seasonality mechanism chosen has the effect of forcing the adults and eggs population densities to oscillate in phase with a period of one year thus mimicking in a schematic way the seasonality in the density of mosquitoes populations.

Another assumption of our model is that the density of adult mosquitoes is checked by the availability of breeding places. We, therefore, assumed that the oviposition rate is dependent on the total eggs density. This is a consequence of competition for limited breeding places in the dry season.

Finally, we assumed that the immature stages between eggs and adults (larvae and pupae) are clumped in a single state called hereafter as 'eggs'.

6. Model's equations

The model describes the dynamics of a vector-borne infection in its three components of transmission, namely, human hosts, mosquitoes and their eggs (the latter includes the intermediate stages, like larvae and pupae). The populations densities, in turn, are divided into susceptible humans, denoted S_H, infected humans, I_H, recovered (and immune) humans, R_H, total humans, $N_H = S_H + I_H + R_H$, susceptible mosquitoes, S_M, infected and latent mosquitoes, L_M, infected and infectious mosquitoes, I_M, non-infected eggs, S_E, and infected eggs, I_E.

The model's dynamics is described by the set of equations.

$$
\begin{aligned}
\frac{dS_H}{dt} &= -ab_H I_M \frac{S_H}{N_H} - \mu_H S_H + r_H N_H \left(1 - \frac{N_H}{k_H}\right)\\
\frac{dI_H}{dt} &= ab_H I_M \frac{S_H}{N_H} - (\mu_H + \alpha_H + \gamma_H) I_H\\
\frac{dR_H}{dt} &= \gamma_H I_H - \mu_H R_H\\
\frac{dS_M}{dt} &= p_S\big(c_S - d_S \sin(2\pi f t + \phi)\big) S_E \theta\big(c_S - d_S \sin(2\pi f t + \phi)\big) - \mu_M S_M - ab_M S_M \frac{I_H}{N_H}\\
\frac{dL_M}{dt} &= ab_M S_M \frac{I_H}{N_H} - e^{-\mu_M \tau_I} a S_M(t-\tau_I) \frac{I_H(t-\tau_I)}{N_H(t-\tau_I)} - \mu_M L_M\\
\frac{dI_M}{dt} &= e^{-\mu_M \tau_I} ab_M S_M(t-\tau_I) \frac{I_H(t-\tau_I)}{N_H(t-\tau_I)} - \mu_M I_M\\
&\quad + p_I\big(c_I - d_I \sin(2\pi f t + \phi)\big) I_E \theta\big(c_I - d_I \sin(2\pi f t + \phi)\big)\\
\frac{dS_E}{dt} &= \big[r_M S_M + (1-g) r_M I_M\big]\left(1 - \frac{(S_E + I_E)}{k_E}\right) - \mu_E S_E\\
&\quad - p_S\big(c_S - d_S \sin(2\pi f t + \phi)\big) S_E \theta\big(c_E - d_E \sin(2\pi f t + \phi)\big)\\
\frac{dI_E}{dt} &= g r_M I_M \left(1 - \frac{(S_E + I_E)}{k_E}\right) - \mu_E I_E\\
&\quad - p_I\big(c_I - d_I \sin(2\pi f t + \pi)\big) I_E \theta\big(c_I - d_I \sin(2\pi f t + \phi)\big)
\end{aligned}
\tag{16}
$$

Let us briefly describe some features of the model.

Susceptible humans grow at the rate $r_H N_H(1 - \frac{N_H}{k_H}) - \mu_H S_H$, where r_H is the birth rate, μ_H is the natural mortality and k_H is related to the human carrying capacity as explained below.

Humans are subject to a density dependent birth rate and a linear mortality rate. The population dynamics in the absence of disease is

$$
\frac{dN_H}{dt} = r_H N_H \left(1 - \frac{N_H}{k_H}\right) - \mu_H N_H, \tag{17}
$$

where r_H is the birth rate of humans, N_H is the total human population, k_H is a constant and the human carrying capacity is $\frac{r_H - \mu_H}{r_H} k_H$.

Note that we are assuming that close to the carrying capacity the human population growth is checked by a reduction in the birth rate. Alternatively the control of the population could be done by a term including density-dependence in the mortality rate and Eq. (17) could be written as

$$
\frac{dN_H}{dt} = r_H N_H - \left(\mu_H + \frac{r_H N_H}{k_H}\right) N_H \tag{18}
$$

which can be interpreted as a density dependence in the mortality rate. However, the net result would be qualitatively the same.

Those susceptible humans who acquire the infection do so at the rate $ab_H I_M \frac{S_H}{N_H}$, where a is the average daily biting rates of mosquitoes and b_H is the fraction of actually infective bites inflicted by infected mosquitoes I_M.

The second equation describes infected humans, I_H, who may either recover, with rate γ, or die from the disease, with rate $(\mu_H + \alpha_H)$.

The third equation describes recovered humans, who remain so for the rest of their lives.

The fourth, fifth and the sixth equations represent the susceptible, latent and infected mosquitos' population densities, respectively. Susceptible mosquitoes vary in size with a time-dependent rate

$$p_S\big(c_S - d_S \sin(2\pi f t + \phi)\big) S_E \theta\big(c_S - d_S \sin(2\pi f t + \phi)\big) - \mu_M S_M \tag{19}$$

The term μ_M is the natural mortality rate of mosquitoes. The term $p_S S_E$ is the fraction of eggs hatching per unit time, and which survived the development through the intermediate stages (larvas and pupas). The time-dependent term $(c_i - d_i \sin(2\pi f t + \phi))\theta(c_i - d_i \sin(2\pi f t + \phi))$ $(i = S, I)$ simulates the seasonal variation in mosquitoes production from eggs, assumed different for infected and susceptible eggs, for generality. By varying c_i and d_i $(i = S, I)$, we can simulate the duration and severity of the winters ($f = 1/365$ days^{-1} and so it fixes one cycle per year). Of course, the parameters determining the length and severity of the seasons should be equal for susceptible and infected eggs and we set them so in the simulations. The Heaviside θ-function (a step function that is equal to zero when the argument is less than zero and one when the argument is greater or equal to zero) $\theta(c_i - d_i \sin(2\pi f t + \phi))$ prevents the term

$$\big(c_i - d_i \sin(2\pi f t + \phi)\big)\theta\big(c_i - d_i \sin(2\pi f t + \phi)\big) \quad (i = S, I) \tag{20}$$

from becoming negative. If c_i is smaller than d_i, then the winter is long and severe. On the other hand, if c_i is greater than d_i, then the winter is short and mild. Those susceptible mosquitoes who acquire the infection do so at the rate $ab_M S_M \frac{I_H}{N_H}$, where a is the average daily biting rates of mosquitoes and b_M is the fraction of bites inflicted by susceptible mosquitoes in infected humans that result in infected mosquitoes. Infected mosquitoes acquire the infection after biting infected humans with a rate $ab_M S_M \frac{I_H}{N_H}$, becoming latent. A fraction of the latent mosquitoes survives the extrinsic incubation period with probability $e^{-\mu_M \tau_I}$ and becomes infective. Therefore, the rate of mosquitoes becoming infective per unit time is $e^{-\mu_M \tau_I} ab_M S_M(t - \tau_I) \frac{I_H(t-\tau_I)}{N_H}$. The probabilities, b_H and b_M, of getting the infection from exposure to infective individuals (either humans or mosquitoes) are not exactly known, but are considered to be close to one [29].

The term

$$p_I\big(c_I - d_I \sin(2\pi f t + \phi)\big) I_E \theta\big(c_I - d_I \sin(2\pi f t + \phi)\big) \tag{21}$$

represents the rate by which infected eggs become infected adults. Infected mosquitoes die at the same rate μ_M as the susceptible ones. The term $p_I I_E$ is the fraction of infected eggs hatching per unit time, and which survived the development through the intermediate stages (larvas and pupas).

The seventh and the eight equations represent the dynamics of susceptible and infected eggs, respectively.

In the seventh equation, the term

$$\big[r_M S_M + (1 - g) r_M I_M\big]\left(1 - \frac{(S_E + I_E)}{k_E}\right) \tag{22}$$

represents the oviposition rate of susceptible eggs born from both susceptible mosquitoes with rate

$$r_M S_M \left(1 - \frac{(S_E + I_E)}{k_E}\right) \tag{23}$$

and from a fraction $(1 - g)$ of infected mosquitoes, with rate

$$(1 - g) r_M I_M \left(1 - \frac{(S_E + I_E)}{k_E}\right) \tag{24}$$

The parameter g, therefore, represents the proportion of infected eggs laid by infected female mosquitoes.

The term $r_M S_M$ represents the maximum oviposition rate of female mosquitoes with the number of viable eggs being checked by the availability of breeding places by the term $(1 - \frac{(S_E + I_E)}{k_E})$. As in the case of humans, the egg's carrying capacity is $\frac{r_E - \mu_E}{r_E} k_E$, where k_E is a constant. Once again we choose density dependence on birth rather than

Table 1
Parameters, biological meaning and their values.

Parameter	Meaning	Value
a	Average daily biting rate	1.2 days^{-1}
b_H, b_M	Fraction of actually infective bites	1
μ_H	Humans natural mortality rate	4×10^{-5} days^{-1}
r_H	Birth rate of humans	2.5 days^{-1}
k_H	Humans carrying capacity	2×10^5
α_H	Dengue induced mortality in humans	10^{-3} days^{-1}
γ_H	Humans recovery rate	0.143 days^{-1}
p_S	Non-infected eggs hatching rate	0.15 days^{-1}
c_S	Climatic factor modulating winters	0.07
d_S	Climatic factor modulating winters	0.06
f	Frequency of the seasonal cycles	2.8×10^{-3} days^{-1}
μ_M	Natural mortality rate of mosquitoes	0.263 days^{-1}
τ	Extrinsic incubation period of dengue	7 days
α_M	Dengue induced mortality in mosquitoes	negligible
r_M	Oviposition rate	50 days^{-1}
p_I	Infected eggs hatching rate	0.15 days^{-1}
c_I	Climatic factor modulating winters	0.07
d_I	Climatic factor modulating winters	0.06
g	Proportion of infected eggs	see text
k_E	Eggs carrying capacity	10^6
μ_E	Natural mortality rate of eggs	0.1 days^{-1}

on death. Again, the control of the population could be done by a term including density-dependence in the mortality rate, but the net result would be qualitatively the same.

Finally, in the last equation the term

$$gr_M I_M\left(1 - \frac{(S_E + I_E)}{k_E}\right) - \mu_E I_E \tag{25}$$

represents the net rate by which infected eggs are produced by infected adult females, that is, vertical transmission of dengue virus.

The phase ϕ will be used to set the rate of eggs' hatching, the adult mosquitos' density and the egg density at their minimum values at $t = 0$.

The biological meaning and the values used in the simulations that follow, of each of the above parameters are shown in Table 1.

7. Entomology without disease

In this subsection we analyze the behavior of the mosquito population density in the absence of disease. This implies that the only equations to be simulated are:

$$\begin{aligned}
\frac{dS_M}{dt} &= p_S\big(c_S - d_S \sin(2\pi f t + \phi)\big) S_E \theta\big(c_S - d_S \sin(2\pi f t + \phi)\big) - \mu_M S_M \\
\frac{dS_E}{dt} &= r_M S_M\left(1 - \frac{S_E}{k_E}\right) - \mu_E S_E \\
&\quad - p_S\big(c_S - d_S \sin(2\pi f t + \phi)\big) S_E \theta\big(c_S - d_S \sin(2\pi f t + \phi)\big)
\end{aligned} \tag{26}$$

This pair of equations follows from Eqs. (16) after making zero all the infected terms. It simulates the annual cycle of mosquitoes breeding. The system of Eqs. (26) is a very simplified model for what is really known about the life cycle of mosquitoes. As mentioned above the immature stages between eggs and adults (larvae and pupae) are clumped in the eggs compartment. It is also an oversimplification of the annual seasons.

The initial conditions and the phase ϕ were chosen such that the density of susceptible mosquitoes ($S_M(0)$), the density of susceptible eggs ($S_E(0)$) and the rate of eggs' hatching are at their minimum. The minimum was determined

by running the program for an arbitrary initial condition (compatible with k_E, and k_H) and setting $\phi = \frac{\pi}{2}$. By doing this we guaranteed that variations in mosquitoes and eggs densities and in eggs' hatching rates are all synchronized (with peaks in 'summer' and troughs in 'winter').

Winters without eggs hatching were simulated by making d_i larger than c_i. This has the effect of making the term $(c_i - d_i \sin(2\pi f t + \phi))$ negative for some parts of the cycle. In these periods the Heaviside function $\theta(c_i - d_i \sin(2\pi f t + \phi))$ makes the hatching of eggs equal to zero, thus reducing the adult forms. If d_i is set smaller than c_i then very weak winters are simulated. Those variations in the length and strength of the winter have the obvious consequence of changing the quality of the summers, although the peak in eggs production in the summer is dependent on the parameter k_E, related to the eggs' carrying capacity. Note that, in the particular case in which $d_i = 0$, we have a threshold in $c_i > \frac{\mu_E \mu_M}{p_S(r_M - \mu_M)}$ $(r_M > \mu_M)$ above which both the eggs and the mosquitoes settle at constant values.

We also checked that the population of mosquitoes survives severe winters through the diapausing of eggs. The density of mosquitoes in the summer following a severe winter can be very large depending on k_E.

8. An approximated threshold condition

In the first part of this section we deduce a threshold condition for epidemic.

We first describe an intuitive approach to get an approximate time-dependent threshold. System (16) has 'no-mass', that is, it responds to perturbations instantaneously. We introduce some disease at time $t = 0$, and 'freeze' the system at time t. At this moment we have infected compartments that we assume to became instantaneously non-infective and investigate the effect of a small amount of infection introduced on the stability of the frozen equilibrium.

Thus we consider a new system of equations consisting of the infective equations of the original system (21), substituting I_H, L_M, I_M, and I_E by i_H, l_M, i_M, and i_E, respectively:

$$\begin{aligned}
\frac{di_H}{dt} &= ab_H \frac{S_H}{N_H} i_M - (\mu_H + \alpha_H + \gamma_H) i_H \\
\frac{dl_M}{dt} &= ab_M \frac{S_M}{N_H} i_H - \mu_M l_M - e^{-\mu_M \tau_I} ab_M \frac{S_M(t-\tau_I)}{N_H(t-\tau_I)} i_H(t-\tau_I) \\
\frac{di_M}{dt} &= e^{-\mu_M \tau_I} ab_M \frac{S_M(t-\tau_I)}{N_H(t-\tau_I)} i_H(t-\tau_I) - \mu_M i_M + p_I\big(c_I - d_I \sin(\Phi)\big) i_E \theta\big(c_I - d_I \sin(\Phi)\big) \\
\frac{di_E}{dt} &= g r_M \left(1 - \frac{(S_E)}{k_E}\right) i_M - \mu_E i_E - p_I\big(c_I - d_I \sin(\Phi)\big) i_E \theta\big(c_I - d_I \sin(\Phi)\big)
\end{aligned} \tag{27}$$

where $\Phi = 2\pi f t + \phi$, and analyze the stability of the trivial solution $i_E = 0$, $l_M = 0$, $i_H = 0$ and $i_M = 0$, as if the system was autonomous [30]. For this we assume the solutions:

$$\begin{aligned}
i_H &= c_1 \exp(\lambda t) \\
l_M &= c_2 \exp(\lambda t) \\
i_M &= c_3 \exp(\lambda t) \\
i_E &= c_4 \exp(\lambda t)
\end{aligned} \tag{28}$$

The characteristic equation associated to system (27) is then obtained:

$$\begin{vmatrix}
-(\lambda + \gamma_H + \alpha_H + \mu_H) & 0 & ab_H \frac{S_H(t)}{N_H(t)} & 0 \\
ab_M \frac{S_M}{N_H} - ab_M e^{(-\mu_M \tau)} \frac{S_M(t-\tau_I)}{N_H(t-\tau_I)} e^{-\lambda\tau} & -(\lambda + \mu_M) & 0 & 0 \\
ab_M e^{(-\mu_M \tau)} \frac{S_M(t-\tau_I)}{N_H(t-\tau_I)} e^{-\lambda\tau} & 0 & -(\lambda + \mu_M) & p_I(c_I - d_I \sin\Phi)\theta(c_I - d_I \sin(\Phi)) \\
0 & 0 & g r_M(1 - \frac{S_E}{k_E}) & -\lambda - \mu_E - p_I(c_I - d_I \sin(\Phi))\theta(c_I - d_I \sin(\Phi))
\end{vmatrix} = 0 \tag{29}$$

If all the roots of Eq. (29) have negative real parts, then the equilibrium without disease is stable, that is, the origin is an attractor. As shown in [15], the first root that crosses the imaginary axis do so through the real axis and this happens when

$$R(t) = \frac{ab_M}{(\gamma_H + \alpha_H + \mu_H)} \frac{S_M(t-\tau_I)}{N_H(t-\tau_I)} \frac{a\exp(-\mu_M\tau)b_H c}{\mu_M} \frac{S_H(t)}{N_H(t)} + \frac{p_I(c_I - d_I\sin\Phi)gr_M\left(1-\frac{S_E(t)}{k_E}\right)\theta(c_I - d_I\sin(\Phi))}{\mu_M(\mu_E + p_I(c_I - d_I\sin\Phi)\theta(c_I - d_I\sin(\Phi)))} > 1 \quad (30)$$

As mentioned above the phase is set at $\phi = \pi/2$ and the initial condition is such that the susceptible mosquito and eggs' densities are at their lowest values.

We claim that (30) is an approximate version of the reproductive number of system (16).

Note that, for small t, the first term in Eq. (30) is exactly the expression proposed in [18] for the so-called basic reproduction number.

We have numerically checked that the time t at which the trivial solution (no-disease) of the autonomous system becomes unstable ($R > 1$) corresponds approximately to the moment at which the epidemic takes off, that is, when the epidemic in system (21) begins to increase as a result of the introduction of a small amount of disease at time $t = 0$.

We also noticed that when introduced successfully the disease shows oscillations and the peaks and troughs of those oscillations correspond approximately to the moments the threshold crosses 1 downwards or upwards, respectively.

9. Understanding the possible behaviors of the system

In the first part of this section we explain the delay observed in disease outbreaks between the peak in mosquito's density and the initial rising in dengue cases. We do so by introducing a small amount of disease into a previously uninfected population when the rate of eggs hatching is at its minimum ($\phi = \pi/2$), and the susceptible mosquito and eggs densities are at their lowest values. In the second part we show how overwintering occurs and discuss and explain the only two different patterns of cyclic outbreaks.

10. Delay in dengue epidemics

It has been observed that aedes population density peaks about one month after the beginning of the rainy season (in southeastern Brazil in the month of October), but dengue epidemics typically appear some three or four months after that. Although our model of seasonality is too crude to fit any data with any degree of accuracy, the delay can be seen in the simulations of the model. In this figure we show the case in which 50% of the hatched eggs from infected females are infected. The average daily men-biting rate, that is, the average per capita biting rate at $t = 0$, $MBR = \frac{S_M(0)}{N_H}a$, was set as 0.63 bites/day and the initial conditions were such that the densities of susceptible mosquitoes ($S_M(0)$) and eggs ($S_E(0)$), and the hatching rate were at their minimum. Then a small amount of disease was introduced. The daily biting rate is of the same order as described in the literature [31,32]. One can note that the mosquito population density drops sharply in the winter (troughs in the traced lines).

The delay between the peak in the mosquito's population density and the peak in dengue epidemics is of the order of 100 days, which corresponds to actual situations in endemic.

Let us try to understand qualitatively the origin of the delay observed in dengue. This is due to the cyclic pattern of the mosquito population density. During the dry season, as mentioned above, the mosquito population density drops to very low levels, below the threshold, $R = 1$, for transmission. In early spring the population density of mosquitoes begins to increase until it reaches a critical level at which the threshold crosses one and transmission begins, thus the delay.

As can be seen from the first term of Eq. (30), this critical level also depends on the fraction of the infected mosquito that survives the extrinsic incubation period with probability $e^{-\mu_M\tau_I}$ and become infective. The longer the extrinsic incubation period, the larger the delay.

11. Dengue overwintering and extinction

In this subsection we begin by testing the hypothesis that the phenomenon of overwintering due to infected mosquito's eggs that survive the dry season. It should be noted that vertical transmission has already been suggested by field studies, in which this effect was considered to be important for *Aedes albopictus* (75% of trans-ovarial transmission described by Shroyer [33]), but less so with *Aedes aegypti* (2.8% of trans-ovarial transmission described by

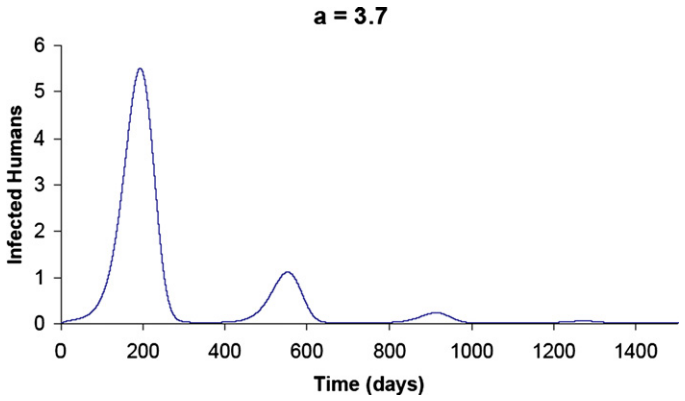

Fig. 1. The first pattern of outbreak, obtained with a value of men-biting rate, $MBR = 0.51$ days^{-1}. One can see a succession of two outbreaks forming a damped oscillation pattern until the disease disappears.

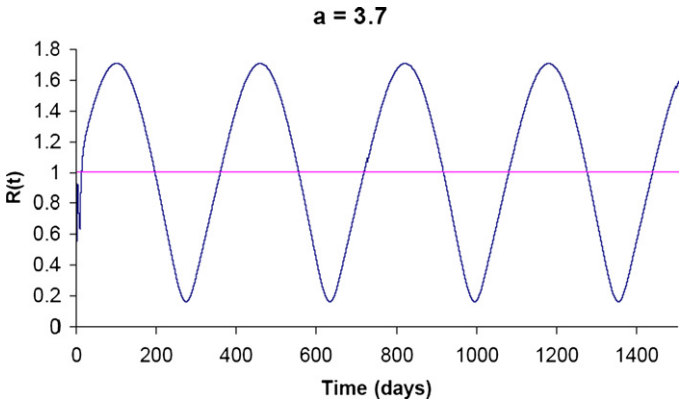

Fig. 2. The threshold $R(t)$ oscillation for the same conditions as Fig. 3. The system oscillates and the time interval during which it is above the threshold for transmission ($R(t) > 1$) is smaller than half of the year.

Joshi et al. [34]). In addition, in a recent publication Crochu et al. [35] demonstrated the incorporation of flavivirus DNA form integrated in the genome of *Aedes spp*. mosquitoes. This may, in the future provide further evidence of vertical transmission.

As it occurs in other vector-borne infections, environmental and climatic conditions, as well as the stock of susceptible humans, determine the existence, intensity and duration of dengue outbreaks. This can be viewed in Figs. 1–6 in which we show and explain two patterns of dengue recurrent outbreaks.

In the first pattern shown in Fig. 1, obtained with a value of men-biting rate, $MBR = 0.51$ days^{-1}, we see a succession of outbreaks forming a damped oscillation pattern until the disease disappears.

This happens because after the summer peak of each outbreak the infection transmission decreases to levels inferior to the ones of the previous cycle. The threshold should be understood as follows: in the time intervals for which $R(t)$ is greater than one, the infection is amplified and in the time intervals for which $R(t)$ is less than one, the infection dies out. Thus, examining Fig. 2 it is possible to understand why the disease disappears. In Fig. 2 we show that the system oscillates and the time interval during which it is above the threshold for transmission ($R(t) > 1$) is smaller than half of the year, that is, the system spends a greater proportion of the year below 1 and this is not enough to keep the virus circulating among hosts. Thus, having $R(t) > 1$ for less than a certain time interval (around 190 days) is not enough to guarantee an epidemic and as small amount of the disease introduced in the time $t = 0$ dies out.

In Fig. 3, we show both the time variation in $R(t)$ and in the total amount of infection, $d(t)$, defined as

$$d(t) = \sqrt{\left(I_H(t)\right)^2 + \left(L_M(t)\right)^2 + \left(I_M(t)\right)^2 + \left(I_E(t)\right)^2} \tag{31}$$

which is the 'distance' to the origin of a point in the orbit $(I_H(t))$, $(L_M(t))$, $(I_M(t))$, $(I_E(t))$.

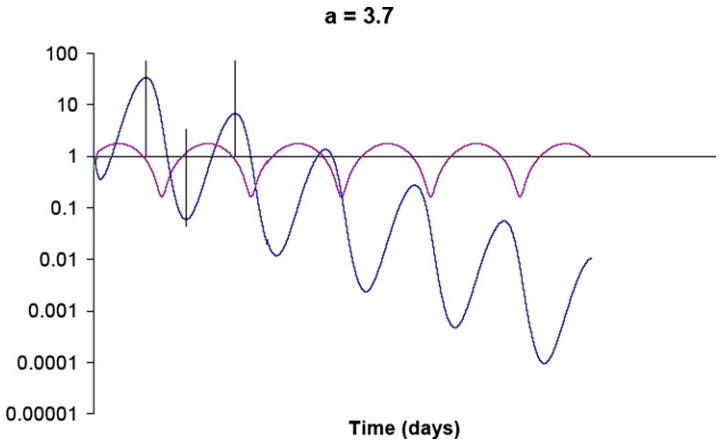

Fig. 3. Both the time variation in $R(t)$ (log scale, purple line) and in the total amount of infection, $d(t)$ (log scale, blue line) with the same conditions as in Fig. 2. It can be noted that the peaks and troughs of $d(t)$ shown occur approximately when $R(t)$ crosses 1, from above downwards and from below upwards, respectively. (For interpretation of the references to color in this figure legend, the reader is referred to the web version of this article.)

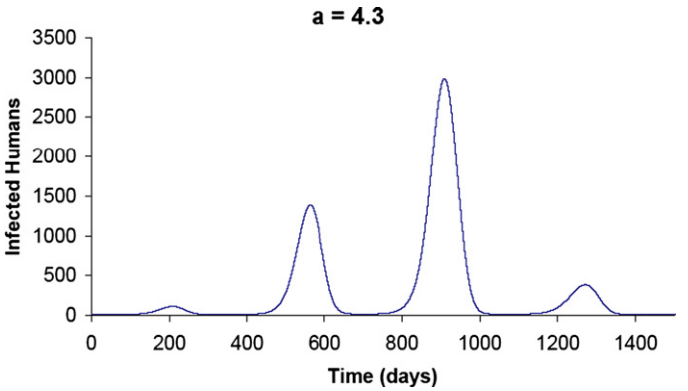

Fig. 4. The second pattern of outbreak, in which $R(t) > 1$ for a greater part of the year in the first outbreaks, was obtained with a value of the men-biting rate $MBR = 0.63$ days^{-1}.

When the infection is disappearing $d(t)$ goes to zero.

It can be noted that the peaks and troughs of $d(t)$ shown in Fig. 3 occur approximately when $R(t)$ crosses 1, from above downwards and from below upwards, respectively.

The second pattern, in which $R(t) > 1$ for a greater part of the year in the first outbreaks, was obtained with a value of the men-biting rate $MBR = 0.63$ days^{-1}. The simulation of the epidemics in this case is shown in Fig. 4.

In this case, the amplitude of the initial outbreaks increases until the fraction of immune individuals reaches a herd immunity threshold and the disease dies out in a damped oscillation pattern. This can be better understood by examining Fig. 6, which shows the time variation of $R(t)$.

In the figure we see that $R(t)$ oscillates and the time interval during which it is above the threshold for transmission ($R(t) > 1$) is larger than half of the year in the first cycles.

In Fig. 6 we show both the time variation in $R(t)$ and in the total amount of infection, $d(t)$, for this case.

Again, it can be noted that the peaks and troughs of $d(t)$ occur approximately when $R(t)$ crosses 1, from above downwards and from below upwards, respectively, and that the effect of herd immunity can be seen by a decrease in the time interval in which $R(t) > 1$.

One important aspect is that the two patterns analyzed above represent the two only epidemiological outcomes of our model, that is, a relatively low intensity of transmission (case 1, Figs. 1–3) and a high intensity of transmission (case 2, Figs. 4–6). In the latter, whenever the intensity of transmission is too high we can have only a single outbreak but this is a particular case of situation 2.

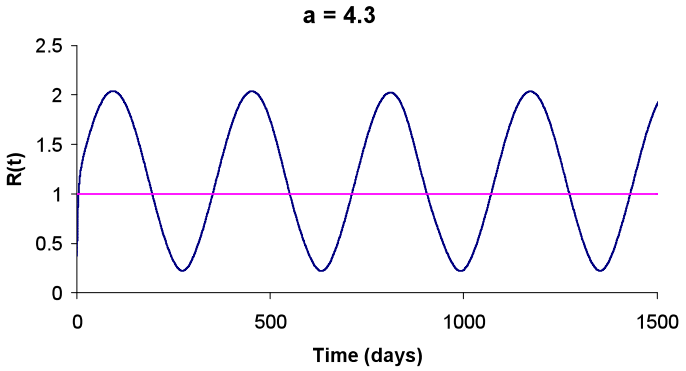

Fig. 5. $R(t)$ oscillation, obtained with the same conditions as in Fig. 4. One can note that the time interval during which it is above the threshold for transmission is larger than one for more than half of the year in the first cycles.

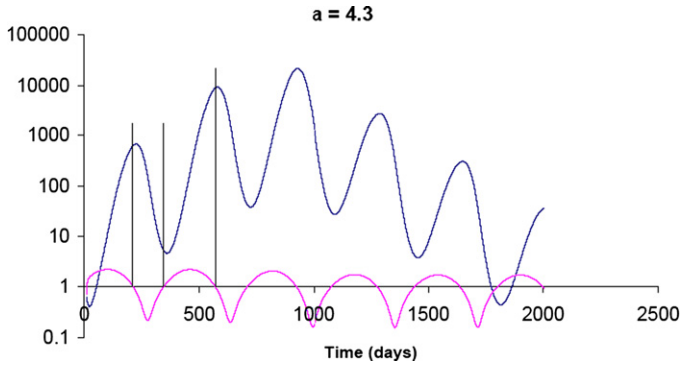

Fig. 6. Both the time variation in $R(t)$ (pink line) and in the total amount of infection, $d(t)$ (blue line), for the same case as in Fig. 4. Again, it can be noted that the peaks and troughs of $d(t)$ occur approximately when $R(t)$ crosses 1, from above downwards and from below upwards, respectively, and that the effect of herd immunity can be seen by a decrease in the time interval in which $R(t) > 1$. (For interpretation of the references to color in this figure legend, the reader is referred to the web version of this article.)

For both patterns the simulation clearly shows the overwintering of dengue epidemics and its disappearance after some time. The proportion of infected eggs was set at $g = 0.5$, a fraction of which $p_I = 0.15$ hatches, evolving into adult females. The product $g \times p_I = 0.075$ is compatible with the proportion of infected eggs described in the literature [31].

Some indirect experimental evidence supports the above results. For instance, as mentioned above, dengue virus strains infecting a less aggressive vector as *Ae. albopictus* must have a high rate of vertical transmission, as shown by [33]. On the other hand, a dengue virus strain infecting a more aggressive vector, as *A. aegypti*, apparently can afford to have a less important vertical transmission [34].

12. The impact of temperature increase on dengue in Singapore [36]

In the period between 1989 and 2005 Singapore observed a steady increase n the ambient temperature (Fig. 7) of around 1 °C. This trend was accompanied by an increase in the number of dengue cases, which increased more than 10-fold in the period.

In what follows we show a model designed to describe the impact of the increase in temperature on dengue in the city of Singapore.

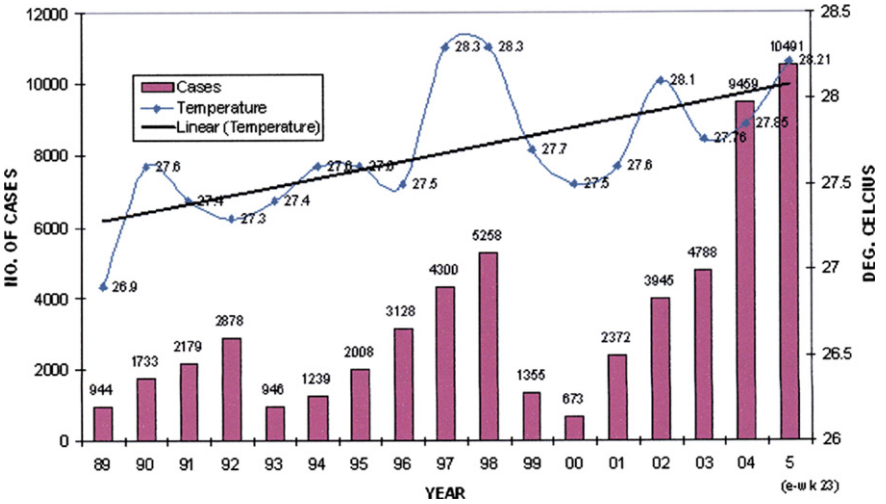

Fig. 7. Ambient temperature and dengue cases in Singapore in the period between 1989 and 2005 (from [37]).

13. The model

Since the seminal attempts of Sir Ronald Ross in applying mathematics to understanding the transmission of malaria, several models to vector-borne infections have been proposed. In what follows we present a dynamical model for dengue transmission based on biological assumptions and on the available data of human cases [17,26].

The model's dynamics is a modified version of the model from [26] and [38].

The structure, that is the number of compartments, transition rates, etc., is the same as the models presented in [26] and [38]. However, there is a very important difference. In the present paper, the average population of mosquitoes is allowed to increase slowly with time. This includes a new variable, which makes the present system non-autonomous in addition to the non-autonomous terms, simulating seasonality presented in the models in [26] and [38].

The model aims to compare the impact of several possible alternative control strategies, which in turn are based on the reproduction number of dengue fever, a threshold condition that will be described in the next section. It also aims to contribute to the understanding of the causes of dengue resurgence to Singapore in the last decade.

The populations involved in the transmission are human hosts, mosquitoes, and their eggs (the latter includes the intermediate stages, like larvae and pupae). The population densities, therefore, are divided in following compartments: susceptible humans, denoted S_H; infected humans, I_H; recovered (and immune) humans, R_H; total humans, N_H; susceptible mosquitoes, S_M; infected and latent mosquitoes, L_M; infected and infectious mosquitoes, I_M; non-infected eggs, S_E; and infected eggs, I_E.

The model's equations are:

$$\frac{dS_H}{dt} = -abI_M\frac{S_H}{N_H} - \mu_H S_H + r_H N_H\left(1 - \frac{N_H}{\kappa_H}\right)$$

$$\frac{dI_H}{dt} = abI_M\frac{S_H}{N_H} - (\mu_H + \alpha_H + \gamma_H)I_H$$

$$\frac{dR_H}{dt} = \gamma_H I_H - \mu_H R_H$$

$$\frac{dS_M}{dt} = p_S c_S(t)S_E - \mu_M S_M - acS_M\frac{I_H}{N_H}$$

$$\frac{dL_M}{dt} = acS_M\frac{I_H}{N_H} - e^{-\mu_M\tau_I}acS_M(t-\tau_I)\frac{I_H(t-\tau_I)}{N_H(t-\tau_I)} - \mu_M L_M$$

$$\frac{dI_M}{dt} = e^{-\mu_M\tau_I}acS_M(t-\tau_I)\frac{I_H(t-\tau_I)}{N_H(t-\tau_I)} - \mu_M I_M + p_I c_S(t)I_E$$

Table 2
The parameters notation, biological meaning and values applied in the simulations [36].

Parameter	Meaning	Value
a	Average daily biting rate	Variable
b_H, b_M	Fraction of actually infective bites	0.6
μ_H	Humans natural mortality rate	3.5×10^{-5} days^{-1}
r_H	Birth rate of humans	2.4×10^{-5} days^{-1}
κ_H	Humans carrying capacity	4×10^5
α_H	Dengue mortality in humans	10^{-3} days^{-1}
γ_H	Humans recovery rate	0.143 days^{-1}
p_S	Susceptible eggs hatching rate	0.15 days^{-1}
d_1	Winter modulation parameter	0.07
d_2	Winter modulation parameter	0.06
f	Frequency of seasonal cycles	2.8×10^{-3} days^{-1}
μ_M	Mosquitoes natural mortality rate	0.263 days^{-1}
τ	Extrinsic incubation period	7 days
α_M	Dengue mortality in mosquitoes	Negligible
r_M	Oviposition rate	50 days^{-1}
p_I	Infected eggs hatching rate	0.15 days^{-1}
g	Proportion of infected eggs	0.5
κ_E	Eggs carrying capacity	As in Eq. (9)
μ_E	Eggs natural mortality rate	0.1 days^{-1}
c	*A. aegypti* susceptibility to dengue	0.54

$$\frac{dS_E}{dt} = \left[r_M S_M + (1-g) r_M I_M\right]\left(1 - \frac{(S_E + I_E)}{\kappa_E}\right) - \mu_E S_E - p_S c_S(t) S_E$$
$$\frac{dI_E}{dt} = [g r_M I_M]\left(1 - \frac{(S_E + I_E)}{\kappa_E}\right) - \mu_E I_E - p_I c_S(t) I_E \tag{32}$$

where $c_S(t) = (d_1 - d_2 \sin(2\pi f t + \phi))$ is a climatic factor mimicking seasonal influences in the mosquito population (see below and Refs. [26,38]). Those and the remaining parameters are explained in Table 2.

Let us briefly describe some features of the model.

Susceptible humans grow at the rate $\{r_H N_H[1 - (N_H/\kappa_H)] - \mu_H S_H\}$, where r_H is the birth rate, μ_H is the natural mortality and k_H is related to the human carrying capacity as explained below.

Humans are subject to a density dependent birth rate and a linear mortality rate. The population dynamics in the absence of disease, as shown in Eq. (17) is

$$\frac{dN_H}{dt} = r_H N_H\left(1 - \frac{N_H}{\kappa_H}\right) - \mu_H N_H \tag{33}$$

where r_H is the birth rate of humans, N_H is the total human population, k_H is a constant and the human carrying capacity is $[(r_H - \mu_H)/r_H]\kappa_H$.

Note that we are assuming that close to the carrying capacity the human population growth is checked by a reduction in the birth rate. Alternatively the control of the population could be done by a term including density-dependence in the mortality rate and Eq. (33) could be written as

$$\frac{dN_H}{dt} = r_H N_H - \left(\mu_H + \frac{r_H N_H}{\kappa_H}\right) N_H \tag{34}$$

which can be interpreted as density dependence in the mortality rate. However, the net result would be qualitatively the same.

Those susceptible humans who acquire the infection do so at the rate $[abI_M(S_H/N_H)]$, where a is the average daily biting rates of mosquitoes and b_H is the fraction of actually infective bites inflicted by infected mosquitoes, I_M.

The second equation of model (32) describes infected humans, I_H, who may either recover, with rate γ, or die from the disease, with rate $(\mu_H + \alpha_H)$.

The third equation of system (32) describes recovered humans, who remain so for the rest of their lives.

The fourth, fifth and the sixth equations of system (32) represent the susceptible, latent and infected mosquitoes population densities, respectively. Susceptible mosquitoes varies in size with a time-dependent rate

$$p_S c_S(t) S_E - \mu_M S_M \tag{35}$$

The term μ_M is the natural mortality rate of mosquitoes. The term $p_S S_E$ is the number of eggs hatching per unit time, and which survived the development through the intermediate stages (larvae and pupae). The term $c_S(t)$ simulates the seasonal variation in mosquitoes production from eggs (see below).

Those susceptible mosquitoes who acquire the infection do so at the rate $[acS_M(I_H/N_H)]$, where a is the average daily biting rates of mosquitoes and c is the fraction of bites inflicted by susceptible mosquitoes in infected humans that result in infected mosquitoes. Infected mosquitoes acquire the infection after biting infected humans with a rate $[acS_M(I_H/N_H)]$, spending some time in a latent period, called the *extrinsic incubation period*. The fraction of those latent mosquitoes that survives the extrinsic incubation period, with a given probability $[\exp(-\mu_M \tau_I)]$ becomes infective. Therefore, the rate of mosquitoes becoming infective per unit time is $[\exp(-\mu_M \tau_I) acS_M(t-\tau_I)(I_H(t-\tau_I)/N_H(t-\tau_I))]$.

The term $p_I I_E$ is the number of infected eggs hatching per unit time, and which survived the development through the intermediate stages (larvae and pupae).

The seventh and the eight equations represent the dynamics of susceptible and infected eggs, respectively.

In the seventh equation, the term

$$\left[r_M S_M + (1-g) r_M I_M\right]\left(1 - \frac{(S_E + I_E)}{\kappa_E}\right) \tag{36}$$

represents the oviposition rate of susceptible eggs born from both susceptible mosquitoes with rate

$$r_M S_M \left(1 - \frac{(S_E + I_E)}{\kappa_E}\right) \tag{37}$$

and from a fraction $(1-g)$ of infected mosquitoes, with rate

$$(1-g) r_M I_M \left(1 - \frac{(S_E + I_E)}{\kappa_E}\right) \tag{38}$$

The parameter g, therefore, represents the proportion of infected eggs laid by infected female mosquitoes.

The term $r_M S_M$ represents the maximum oviposition rate of female mosquitoes with the number of viable eggs being checked by the availability of breeding places by the term $\{1 - [(S_E + I_E)/\kappa_E]\}$. As in the case of humans, the egg's carrying capacity is $[(r_E - \mu_E)/r_E]\kappa_E$, where κ_E varies with time, as discussed and described below in Eq. (40). Once again we choose a density dependence on birth rather than on death. Again, the control of the population could be done by a term including density-dependence in the mortality rate, but the net result would be qualitatively the same.

Finally, in the last equation the term

$$[g r_M I_M]\left(1 - \frac{(S_E + I_E)}{\kappa_E}\right) \tag{39}$$

represents the net rate by which infected eggs are produced by infected adult females, that is, vertical transmission of dengue virus.

14. Model's simulations

As mentioned above, in the fifteen years between 1989 and 2005 the temperature in Singapore increased linearly [37]. This increase in the temperature, in turn, is significantly correlated with the increase in the number of dengue cases (see Fig. 7).

We, therefore, assumed that this increase in the local temperature was responsible for an increase in the breeding conditions of *Aedes* mosquitoes, which can be simulated by a linear increase in the carrying capacity, κ_E such that:

$$\kappa_E(t) = \kappa_E(0) + \varepsilon t \tag{40}$$

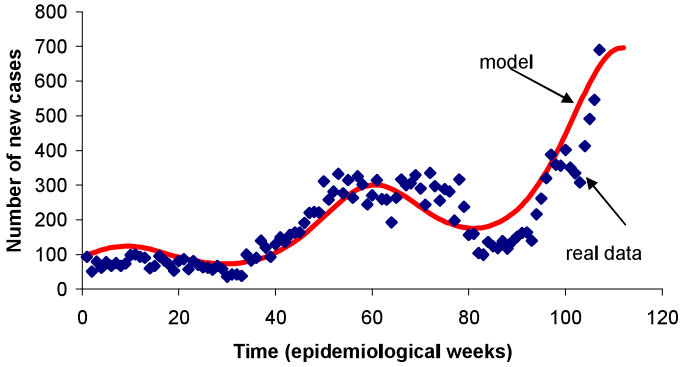

Fig. 8. Result of the model's simulation (red line) as compared with real data (blue diamonds). (For interpretation of the references to color in this figure legend, the reader is referred to the web version of this article.)

To simulate seasonal variations in a schematic way we assumed:

$$c_S(t) \to \big(d_1 - d_2 \sin(2\pi f t + \phi)\big)\theta\big(d_1 - d_2 \sin(2\pi f t + \phi)\big), \quad d_1 \text{ and } d_2 \geqslant 0 \tag{41}$$

where θ is the Heaviside function. The meaning of this substitution is that we assumed that the hatching rate of the eggs varies along the year being low in the 'winter' (low transmission season) and high in the 'summer' (high transmission season). To understand this, note that when d_1 is less than d_2, the θ function makes this rate to vanish for a period during the 'winter'. If d_2 is less than d_1 then the 'winter' is mild. When $d_2 = 0$ there is no seasonality. The term f is the frequency with which high and low transmission seasons alternate. Finally, the parameter ϕ is used to synchronize the population of mosquitoes so that it reaches a minimum when the hatching rate is also at minimum.

The result of the model's simulation for the 2004–2005 epidemic can be observed in Fig. 8.

We can see that the model tallies with the actual data with reasonable accuracy. Actually, we did not intend to fit the model to the data but rather to reproduce qualitatively the trend in the number of cases observed in the last years. The parameters notation, biological meaning and values applied in the simulations are shown in Table 2.

15. The threshold for transmission

A time-dependent threshold condition for transmission can be deduced from the model's equations [26,38] and results in the following equation:

$$R(t) = \frac{ab}{(\mu_H + \alpha_H + \gamma_H)} \frac{ace^{-\mu_M \tau_I}}{\mu_M} \frac{N_M(t-\tau_I)}{N_H(t-\tau_I)} \frac{S_H(t)}{N_H(t)} + \frac{p_I c_I(t) g r_M \big(1 - \frac{S_E(t)}{\kappa_E}\big)}{\mu_M(\mu_E + p_I c_I(t))} > 1 \tag{42}$$

The first term of the equation, evaluated at $t = 0$, is the Macdonald equation [18]. The second term comes from the model's terms related to immature stages as an important contributor for the epidemic.

With this model we can simulate the impact on dengue outbreaks of four different control strategies, namely, killing adult mosquitoes (adulticide), killing immature stages (larvicide), preventing contact between infected humans and vectors (quarantine) and combinations of the first two (mixed).

The first strategy can be implemented in the model by increasing the parameter μ_M, the mosquito's mortality rate; the second strategy can be simulated by increasing the parameter μ_E, the immature stages mortality rate; the third strategy can be simulated by reducing the product ac, that is, by simulating a reduction in the contact between infected humans and susceptible vectors. Finally, the mixed strategies can be simulated by a combination of the first two that is, by reducing μ_M and μ_E in different proportions.

16. Sensitivity analysis

In order to estimate the impact of alternative strategies we carried out a sensitivity analysis of the reproduction number to the following parameters: *biting rate, the product of the parameters a and c, eggs carrying capacity, mosquitoes mortality rate* and *immature states mortality rate*. The choice of these parameters was related to the theoretical possibility of control. So, the biting rate could be reduced by methods that avoid the contact between humans and mosquitoes, like bed nets, use of repellents, etc. The eggs carrying capacity can be reduced by the set of methods called "source reduction", consisting in destroying breeding places. The mosquito's mortality rates can be increased by the use of adulticides. Finally, the immature states mortality rate can be reduced by the application of larvicides.

The results are:

$$\frac{\partial R}{\partial a} = 2\frac{abc}{(\mu_H+\alpha_H+\gamma_H)}\frac{N_M(t-\tau_I)}{N_H(t-\tau_I)}\frac{e^{-\mu_M\tau_I}}{\mu_M} \tag{43}$$

$$\frac{\partial R}{\partial ac} = \frac{ab}{(\mu_H+\alpha_H+\gamma_H)}\frac{N_M(t-\tau_I)}{N_H(t-\tau_I)}\frac{e^{-\mu_M\tau_I}}{\mu_M} \tag{44}$$

$$\frac{\partial R}{\partial \kappa_E} = \frac{p_I c_I(t) g r_M S_E}{\mu_M(\mu_E+p_I c_I(t))\kappa_E^2} \tag{45}$$

$$\begin{aligned}\frac{\partial R}{\partial \mu_M} = &-\frac{\tau_I a}{(\mu_H+\alpha_H+\gamma_H)}\frac{N_M(t-\tau_I)}{N_H(t-\tau_I)}\frac{ae^{-\mu_M\tau_I}bc}{\mu_M}\\ &-\frac{a}{(\mu_H+\alpha_H+\gamma_H)\mu_M^2}\frac{N_M(t-\tau_I)}{N_H(t-\tau_I)}\frac{ae^{-\mu_M\tau_I}bc}{\mu_M}\\ &-\frac{\tau_I e^{-\mu_M\tau_I}p_I c_I(t) g r_M\left(1-\frac{S_E}{\kappa_E}\right)}{\mu_M^2(\mu_E+p_I c_I(t))}\end{aligned} \tag{46}$$

$$\frac{\partial R}{\partial \mu_E} = -\frac{p_I c_I(t) g r_M\left(1-\frac{S_E}{\kappa_E}\right)}{\mu_M(\mu_E+p_I c_I(t))^2} \tag{47}$$

The parameter to which the model seems to be most sensitive is the daily mortality rate of adult mosquitoes. This was numerically confirmed.

17. The impact of temperature on the mosquito-vectors' life cycle [39]

Many factors relevant to the transmission of vector-borne pathogens are highly temperature-dependent. For the invertebrate vector, these include: spatial distribution, development and survivorship rates, and length of gonotrophic cycle (time between meals). For the pathogen itself, temperature affects both the extrinsic incubation period (time from infection of the vector to transmission of the pathogen) and the transmission rates. The effects of temperature on pathogen transmission have been studied most for mosquito-borne pathogens, notably those causing malaria and viral encephalitis [40]. In this section we describe how we calculated the implications of increase in temperature on malaria risk of transmission by applying mathematical models to the mosquito life cycle and the infection transmission. Temperatures referred to in the model are the air temperature for adult mosquitoes and their habits, and water temperature for the eggs, larvae and pupae. We assumed, therefore, that an increase in average temperature in a region will be correlated with increases in the microhabitat temperatures experienced by the mosquitoes.

18. Mosquito life cycle parameters

The rate of all metabolic processes in insects is directly dependent on the environmental temperature [41]. Therefore, its is, in principle, possible to establish mathematical functions that relate each of those rates (including parasite development) with temperature. Not all of them, however, have been studied in enough detail, at least for the same mosquito species. Prochnow [42,43] was the first author to discuss the velocity curve of insect development as a function of temperature. He drew curves for each insect species studied and constructed an average curve of development

Table 3
Mosquito and parasite parameter functions of temperature [38].

Parameter	Function
Man-biting rate $a(T)$	$(15.19e^{-0.041T})^{-1} \times HBI$
Egg hatching rate $\alpha(T)$	$(1.99 + e^{6.26-0.29T})^{-1}$
Pupal development rate $\beta(T)$	$(3.56 + e^{4.5-0.16T})^{-1}$
Adult emergence rate $\gamma(T)$	$(0.88 + e^{3.97-0.16T})^{-1}$
Adult mortality rate $\mu_A(T)$	$(121.97 + e^{5.5-0.019T})^{-1}$
Female fertility $\Phi(T)$	$600 \times \mu_A(T)$
Extrinsic incubation period $n(T)$	$(7.75 + e^{7.77-0.27T})$

velocities as dependent on temperature, which presents the following features: the velocity of development increases at first slowly up to 15 °C; then the acceleration becomes more rapid, but close to the peak of the curve at around 28 °C a falling off of the velocity becomes evident. Beyond the point of the maximum velocity the curve descends steeply. This is, unfortunately, one of the very few articles dealing with the problem of insect abundance as a function of temperature.

As this section is centered on the malaria problem, we concentrate our attention on anopheline species. The following mosquito life cycle parameters were estimated: the biting rate of the vector, a; adult female fertility (number of eggs laid per blood meal), Φ; the rate of development of larvae from eggs, α; eggs mortality rate, μ_E; the rate of pupa development from larvae, β; larval mortality rate, μ_L; the rate of adult development from pupae, γ; pupa mortality rate μ_P; the adults mortality rate, μ_A; and the extrinsic incubation period for plasmodia, n. Density-dependent regulatory processes were considered by assuming a constraint represented by stage-specific carrying capacities, κ.

The biting rate of the vector, a, was calculated as a function of environmental temperature, $a(T)$, from the fact that blood digestion is accelerated by a rise in temperature. So, for *Anopheles braziliensis* (*pessoai*), for instance, eggs are laid a day sooner at 30 °C than for 25 °C [44]. We then fitted a continuous function for these data, which relates the interval between blood meals and temperature. The vector biting rate results from the division of the human blood index (HBI), the proportion of captured female that contain blood in their stomach, by the gonotrophic cycle (feeding interval) [45]. For *Anopheles quadrimaculatus*, for instance, HBI is estimated to be around 40 °C in some regions [46]. The female fertility, Φ, was calculated by assuming that the metabolic processes increase with temperature. Therefore, it is expected that the number of eggs laid per female as a function of temperature, $\Phi(T)$, should follow an indicator of the metabolic rate. Actually, any external factor may influence the fertility of an insect in two different ways. First, it may affect the rate of development of the gonads in the insect body. Second, the mechanism by which the mature eggs are deposited may also be directly influenced. Mayne [47] found that, for *Anopheles quadrimaculatus* the eggs are laid at 12.8–16.7 °C, but not at 4.4–12.2 °C. Bishop [48] found that, for the house-fly, the length of the pre-oviposition period may vary from four days at 10.6 °C to 20 days at 20 °C, a five-fold increase. Schubert [49] also found a five-fold increase in fertility rates of *Priesma quadratum* with the increase of 10 degrees in temperature. We, therefore, chose the adult mortality rate as an indicator of the metabolic rate based on the finding of Rose and Charleworth [50], whose experiments with flies of the genus *Drosophila* demonstrated an inverse correlation between longevity and fecundity. The resultant fertility rates increase five-fold with 10 degrees in temperature increase. Eggs, μ_E, larval, μ_L, and pupal, μ_P, mortality rates were kept as invariants with temperature due to the lack of data on such rates. The rate of eggs hatching, α, the rate of pupal development, β, and the rate of adult emergence, γ, were calculated as functions of temperature $\alpha(T)$, $\beta(T)n$ and $\gamma(T)$, from data for *Anopheles minimus* described in Thomson [51]. Adult mortality rate μ_A, as a function of temperature, $\mu_A(T)$, was calculated from data of Russel and Rao [52] for *Anopheles culicifacies*. The last parameter fitted to temperature variation was the length of the extrinsic incubation period, n, calculated from data described in Stratman-Thomas [53], who made a careful study of the effect of different temperature conditions on the course of infection of *Anopheles quadrimaculatus* with *Plasmodium vivax*. Table 3 shows the fitting functions for each of the parameters studied.

19. A model for the mosquito life cycle

To estimate the relative abundance of adult mosquitoes as a function of environmental temperature we designed a mathematical model, which is intended to mimic the mosquitoes' life cycle. The model is deterministic and as-

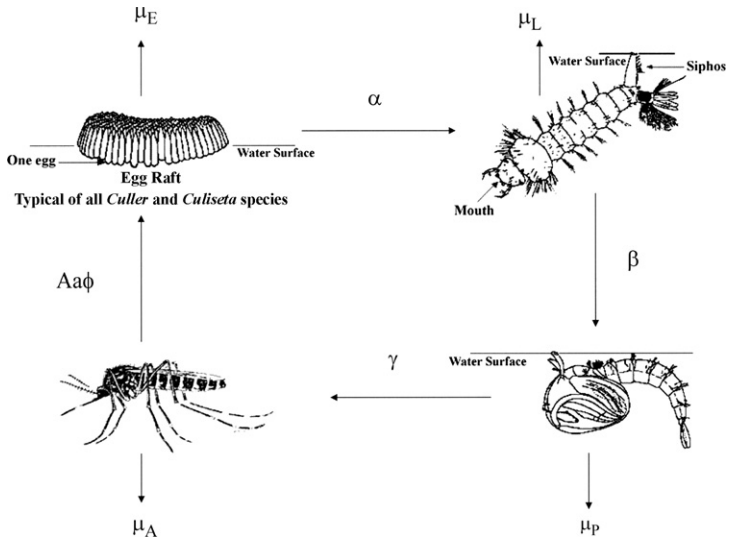

Fig. 9.

sumes the transition rates as functions of temperature, as described above. The life cycle is divided into four stages: eggs, denoted $E(t,T)$; larvae (we assumed only one larval stage although we are aware of the four larval stages of mosquitoes), denoted $L(t,T)$; pupae, denoted $P(t,T)$; and the adult phase, denoted $A(t,T)$. Fig. 9 shows the mosquitoes' life cycle assumed by the model.

The model is expressed by the following system of partial differential equations:

$$\begin{aligned}
\frac{\partial E(t,T)}{\partial t}+\frac{\partial E(t,T)}{\partial T}&=\big[A(t,T)a(t,T)\phi(T)-\big(\alpha(T)+\mu_E\big)E(t,T)\big]\bigg[1-\frac{E(t,T)}{\kappa_E}\bigg]\\
\frac{\partial L(t,T)}{\partial t}+\frac{\partial L(t,T)}{\partial T}&=\big[a(t,T)E(t,T)-\big(\beta(T)+\mu_L\big)L(t,T)\big]\bigg[1-\frac{L(t,T)}{\kappa_L}\bigg]\\
\frac{\partial P(t,T)}{\partial t}+\frac{\partial P(t,T)}{\partial T}&=\big[\beta(t,T)L(t,T)-\big(\gamma(T)+\mu_P\big)P(t,T)\big]\bigg[1-\frac{P(t,T)}{\kappa_P}\bigg]\\
\frac{\partial A(t,T)}{\partial t}+\frac{\partial A(t,T)}{\partial T}&=\big[\gamma(t,T)P(t,T)-\mu_A A(t,T)\big]\bigg[1-\frac{A(t,T)}{\kappa_A}\bigg]
\end{aligned}\tag{48}$$

where t stands for time and T for temperature. The last terms in the equations were included in order to account for stage-specific density dependence.

The model above was numerically simulated for every degree of temperature variation in the parameters, in order to estimate the density of adult females at the system's equilibrium. The number of adult females reached at equilibrium for each degree of temperature variation, $A^*(T)$ allowed us to estimate the relative density of mosquitoes, $m(T)$, which in turn was used for the calculation of the basic reproduction number $R_0(T)$.

20. A model for malaria transmission [54]

The relative increase in the risk of malaria as a result of the average increase in atmospheric temperature was estimated through a dynamical model described in details in [54]. This model assumes the total human population divided into four compartments, namely, susceptibles, infected but yet seronegatives, infected seropositives, and immunes, represented by $X(t,T)$, $Y(t,T)$, $Y'(t,T)$, and $Z(t,T)$, respectively.

The compartments $Y(t,T)$ and $Y'(t,T)$ represent the 'parasite positive' fraction of the population (prevalence) and $Y'(t,T)$, and $Z(t,T)$ represent the fraction of the population with malaria antibodies detectable in a serological test (seroprevalence). Hence, people in $Y'(t,T)$ are both parasite positive and seropositive.

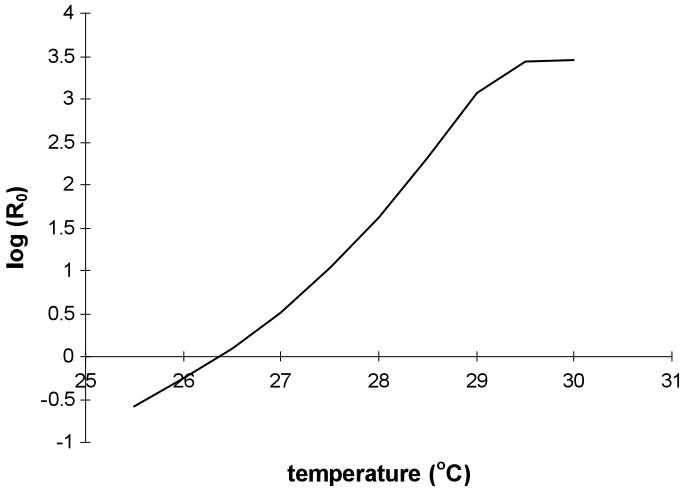

Fig. 10. Logarithm of the basic reproduction number as a function of temperature. The threshold for transmission $R_0(T) = 1$ is surpassed for temperature around 26.5 °C.

The model has a dynamic represented by the following set of partial differential equations:

$$\begin{aligned}
&\frac{\partial X(t,T)}{\partial t} + \frac{\partial X(t,T)}{\partial T} = -h(T)X(t,T) + rY(t,T) + \sigma Z(t,T)\\
&\frac{\partial Y(t,T)}{\partial t} + \frac{\partial Y(t,T)}{\partial T} = h(T)X(t,T) - (r+\delta)Y(t,T)\\
&\frac{\partial Y'(t,T)}{\partial t} + \frac{\partial Y'(t,T)}{\partial T} = \delta Y(t,T) - \varphi Y'(t,T)\\
&\frac{\partial Z(t,T)}{\partial t} + \frac{\partial Z(t,T)}{\partial T} = \varphi Y'(t,T) - \sigma Z(t,T)
\end{aligned} \tag{49}$$

Here $h(T)$ is the temperature-dependent force of infection, and the remaining rates are described in detail in [54]. The model was then numerically simulated until it reached the equilibrium. Finally, malaria prevalence was then related to environmental temperature.

For the estimation of the temperature-dependent force of infection, $h(T)$, we calculated the temperature-dependent basic reproduction number $R_0(T)$ from Eq. (1) with the parameters as follows. The density of adult mosquitoes females, $m(T)$, resulted from the model for mosquito life cycle; the man-biting habits, $a(T)$, were estimated according to Table 3; the proportion of effectively infective females, b, was set as equal to 1%; the parasitemia recovery rate, r, was set as equal to 20 days^{-1}; the mosquito's mortality rate, $\mu(T)$; and the extrinsic incubation period $n(T)$, as in Table 3. The result of those estimations can be seen in Fig. 10.

It can be seen from the figure that the threshold for the persistence of the infection $R_0(T) = 1$ is surpassed for temperature around 26.5 °C.

The proportion of infected individuals resultant from the simulation of the malaria model is shown in Fig. 11.

It can be noted that the infected fraction of the host population is zero below the threshold temperature of just above 26.5 °C. This is in accord with the calculation of $R_0(T)$. After the threshold temperature, the epidemic is triggered and the infected proportion increases steeply until it reaches a maximum value around 30 °C. In addition, it is possible to conclude that the proportion of malarial cases increases more than 10 times with the increase of only 2 °C in temperature in the range above the threshold.

The existence of a temperature threshold does not imply that it represents a lower limit for the existence of malaria. It is a limit for the establishment of endemic malaria. In fact, in many places malaria is epidemic with temperatures below that threshold.

This section should be viewed as an essay on the effects of a theoretical possibility, namely, that a global increase in the atmospheric temperature is related to the spread of tropical infections transmitted by blood-sucking insects.

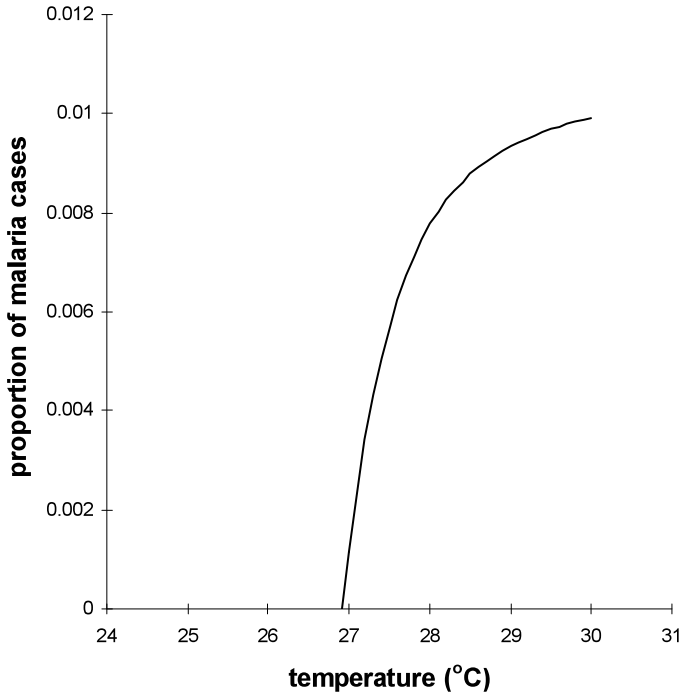

Fig. 11. Proportion of malaria as a function of temperature. There is a clear threshold for the establishment of the disease.

In spite of some theoretical progress represented by the above estimations, we are still many steps away from the ecology of diseases. Epidemiology is far more ecological a topic than mere physiological projections can cope with, and range extension is a problem of dynamic biogeography rather than the mapping of threshold temperatures. Knowledge of the physiological responses of the vectors to temperature is an important component of the analysis but is clearly no substitute for the ecological and biogeographic analysis. On the other hand, when information is not available, one role of a model is to indicate which information has to be gathered.

21. The impact of temperature in the evolution of parasite virulence

The evolution of virulence has been the subject of formal analysis for decades [55–63]. Theoretical work has shown that parasites should evolve intermediate levels of virulence [55,56,64–67]. These intermediate levels of virulence have been attributed to a tradeoff between intra-host replication by the parasite and the negative effect that such replication has on inter-host transmission [62]. In cases where intra-host replication increases the host mortality, virulence tends to decrease, whereas virulence tends to increase in cases where intra-host replication results in higher transmissibility [56].

The ecology of virulence, in particular the impact of climatic factors on parasite virulence [62,68], has received little attention. In the case of vector-borne infections, climate has been suggested as the most significant driver of disease [68]. This is particularly significant nowadays when important global changes in temperature are occurring at a dramatic rate [68].

However, the impact of an increase in temperature on the virulence of vector-borne parasites is still unknown.

We propose a model to evaluate the impact of temperature increase on the evolution of virulence. The model is intended to answer the question of which combination of environmental temperature T and virulence υ maximizes $R_0(T, \upsilon)$. This is based on the assumption that the strain with the highest R_0 is evolutionarily stable [67]. For this, we calculate the tangent plane to the maximum point, that is $\partial R_0/\partial T = 0$ and $\partial R_0/\partial \upsilon = 0$ [61]. The model proposes that an increase in temperature is associated with an increase in parasite virulence.

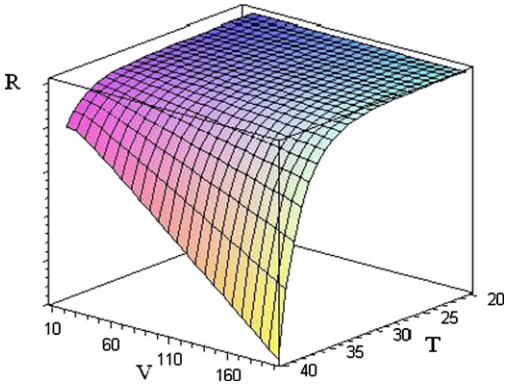

Fig. 12. The reproductive ratio as a function of temperature and virulence in the case when there exists a tangent plane that maximizes it.

22. The model

The model is designed for a vector-borne infection [69,70] and assumes that the transmission parameter is dependent on the temperature and that the removal rate is dependent on parasite virulence, defined as the capacity of the parasite to replicate within the host. The exception is the probability of a vector acquiring the infection from an infectious host, which is assumed to be dependent on the parasitemia; that is, virulence. Virulence is generally defined as the decrease in Host fitness [71]. Here we assume virulence as the capacity of the parasite to replicate within the host in the sense that the more virulent the parasite strain, the higher the parasitemia. This is assumed to be directly related to the instantaneous mortality rate, and indirectly related to the recovery rate from parasitemia.

Let us consider the expected lifetime production of new infections generated by a single infected host per susceptible host in the population, which is Dieckmann's [72] reproductive value, R

$$R = \int_0^\infty \beta(T,\upsilon,s)\exp\left[-\int_0^s u(T,\upsilon,r)\,dr\right]ds \tag{50}$$

where $\beta(T,\upsilon,s)$ is the transmission rate, dependent on the temperature, T, virulence, υ, and age of the infection, s, and $u(T,\upsilon,s)$ is the removal rate from the infectious condition, dependent on the same variables. In what follows we consider the case in which R is independent on the age of infection, which simplifies our analysis.

Suppose that two strains of a given parasite are competing for the same host. It is possible to demonstrate [59] that the strain with an evolutionary stable strategy succeeds, that is, the one that wins the competition is the one with the largest value of R. We want to know which function combining temperature T and virulence υ maximizes R. For this, we assume that there is a tangent plane to the maximum point, that is, the parasite's evolutionarily stable strategy, as in Fig. 12.

For this, we take [59]:

$$\frac{\partial R}{\partial T} = 0 \tag{51}$$

and

$$\frac{\partial R}{\partial \upsilon} = 0 \tag{52}$$

Now, let us consider the case of a vector-borne infection. In this case the transmission rate is

$$\beta(T,\upsilon) = m(T)a^2(T)b\exp\bigl(-\mu_M(T)\tau(T)\bigr)c(\upsilon)/\mu(T) \tag{53}$$

and the removal rate from the infectious condition is

$$u(\upsilon) = \bigl[\alpha_H(\upsilon) + \gamma_H(\upsilon)\bigr] \tag{54}$$

Here, as before, m is the density of mosquitoes as related to humans, a is the average daily biting rate of the vector, b is the fraction of actually infective bites to humans, α_H is the disease induced mortality rate in humans, γ_H is the human recovery rate from the infection, c is the fraction of actually infective bites to mosquitoes, μ is the natural mortality rate of mosquitoes, and τ is the extrinsic incubation period of the parasite.

Note that, for the sake of generality, we consider the infectious terms as dependent on the temperature, except for the probabilities of infection to humans, b, and to mosquitoes, $c(\upsilon)$, the latter being dependent on virulence υ. In addition, the removal rate from the infectious condition is composed of terms dependent on virulence υ.

The mosquitoes' density, m, is a well-known parameter that is strongly dependent on the environmental temperature, insofar as the higher the temperature, the greater the abundance of mosquitoes, up to a certain maximum temperature [39]. The mosquitoes' daily average biting rate, a, was also assumed to be a function of environmental temperature, based on the fact that blood digestion is accelerated by a rise in temperature [44]. Adult mosquitoes' mortality rate as a function of temperature, $\mu(T)$, was based on work by Russel and Rao [52], who demonstrated a linear increase in mosquitoes' mortality. The extrinsic incubation period, τ, is a parameter known since the 1940s to be strongly dependent on temperature [53]. Finally, the probability of infection to mosquitoes, c, was assumed to be dependent on virulence based on the fact that higher parasite virulence is an inevitable consequence of higher rates of reproduction within the host and, therefore, higher parasitemia, thus making a higher concentration of inoculate available for the vectors [59].

The term for removal from the infectious condition (Eq. (54)) has all its terms dependent on virulence. This is based on the assumption that higher parasitemia causes higher mortality to hosts, α, and lower recovery rates from the infection, γ.

Now, from the simplified version of Eqs. (50) and (51), we have:

$$\frac{\partial}{\partial T}\int_0^\infty \beta(T,\upsilon)e^{-\int_0^s u(T,\upsilon,r)\,dr}\,ds = \frac{\partial\beta(T,\upsilon)/\partial T}{\beta(T,\upsilon)} - \int_0^s \frac{\partial u(T,\upsilon,r)}{\partial T}\,dr = 0 \tag{55}$$

or

$$\begin{aligned}\frac{\partial}{\partial T}\int_0^\infty \beta(T,\upsilon)\exp\left[-\int_0^s u(T,\upsilon,r)\,dr\right]ds = {}& \frac{2}{a(T)}\frac{\partial a(T)}{\partial T} + \frac{1}{m(T)}\frac{\partial m(T)}{\partial T} \\ & - \left[\tau(T) + \frac{1}{\mu(T)}\right]\frac{\partial\mu(T)}{\partial T} \\ & - \mu(T)\frac{\partial\tau(T)}{\partial T} = 0\end{aligned} \tag{56}$$

In addition, from (50) and (52), we have:

$$\begin{aligned}\frac{\partial}{\partial \upsilon}\int_0^\infty \beta(T,\upsilon)\exp\left[-\int_0^s u(T,\upsilon,r)\,dr\right]ds = {}& \frac{\partial c(\upsilon)/\partial\upsilon}{c(\upsilon)} \\ & - \left\{\frac{1}{[\alpha_H(\upsilon)+\gamma_H(\upsilon)]}\right. \\ & \left.\times\left[\frac{\partial\alpha(\upsilon)}{\partial\upsilon} + \frac{\partial\gamma(\upsilon)}{\partial\upsilon}\right]\right\} = 0\end{aligned} \tag{57}$$

In this case, from Eqs. (51) and (52), we equate Eqs. (56) and (57), such that:

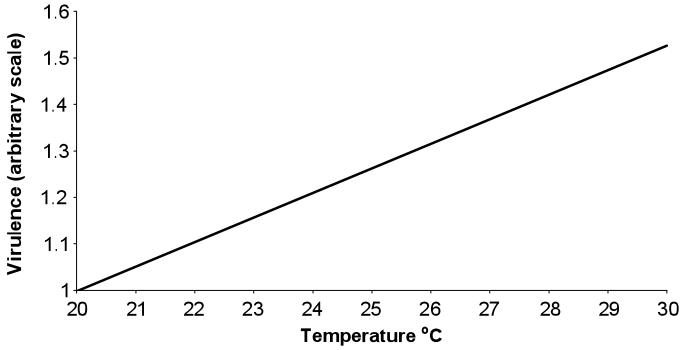

Fig. 13. Solution of Eq. (60).

$$\frac{2}{a(T)}\frac{\partial a(T)}{\partial T} + \frac{\partial m(T)}{\partial T}\frac{1}{m(T)} - \mu(T)\frac{\partial \tau(T)}{\partial T} - \left[\tau(T) + \frac{1}{\mu(T)}\right]\frac{\partial \mu(T)}{\partial T} = \frac{\partial c(\upsilon)/\partial \upsilon}{c(\upsilon)} - \left\{\frac{1}{\alpha_H(\upsilon) + \gamma_H(\upsilon)} \times \left[\frac{\partial \alpha(\upsilon)}{\partial \upsilon} + \frac{\partial \gamma(\upsilon)}{\partial \upsilon}\right]\right\} \tag{58}$$

Again, for simplicity, based on the assumptions stated above of the dependence of the parameters on T and υ, let us assume the following functional relationships (from the parameters of R_0 as proposed by Macdonald [18]):

$$\begin{aligned} m(T) &= \kappa_1\left[1 - \exp(-\kappa_2 T)\right] \\ c(\upsilon) &= \kappa_3 \upsilon^2 \\ \alpha_H(\upsilon) &= \kappa_4 \upsilon \\ \gamma_H(\upsilon) &= \gamma_0 - \kappa_5 \upsilon \\ \mu(T) &= \kappa_6 T \\ \tau(T) &= \tau_0 - \kappa_7 T \\ a(T) &= \kappa_8 T \end{aligned} \tag{59}$$

Therefore, from (58) and (59), we have:

$$\upsilon = \frac{\frac{2}{T} + \frac{\kappa_2 e^{-\kappa_2 T} T + 2\kappa_6\kappa_7 T^2(1-e^{-\kappa_2 T}) - (1-e^{-\kappa_2 T})}{(1-e^{-\kappa_2 T})T} - 2\gamma_0}{\kappa_4 - \kappa_5} \tag{60}$$

which is an explicit relationship between υ and T. Remember that Eq. (50) is a functional relationship between υ and T that maximizes R assuming (53) and (54). That is, in the plane comprised by Eqs. (50)–(52), there is a functional relationship between υ and T whose shape is given by Eq. (60).

23. The simplest case

As the value of the parameters κ are not known we set them all as equal to 1 (we made κ_4 slightly higher than κ_5 to avoid division by zero in Eq. (60)).

In Fig. 13, we see the solution of Eq. (60) with the parameters as above.

By simply examining Eq. (60), we note that the shape displayed in Fig. 13 could be inferred from that equation, since the numerator is an increasing function of T. However, it must be assumed that the relative impact of temperature must be greater on the mortality rate than on the recovery rate ($\kappa_4 > \kappa_5$), such that an increase in temperature is associated with an increase in parasite virulence.

Table 4
Values of the parameters composing Eq. (5).

Parameter	Value
c_0	1
α_0	2×10^{-1}
γ_0	10^{-1}
a_0	5
m_0	10^5
μ_0	10^{-1}
τ_0	5
κ_1	8×10^{-2}
κ_2	10^{-1}
κ_3	10^{-2}
κ_4	10^{-2}
κ_5	10^{-5}
κ_6	5×10^{-1}
κ_7	10^{-2}

24. A more realistic case

In the simplest case analysed above we assumed the existence of a tangent plane that could describe $R_0(T, \upsilon)$ maximized by both temperature and virulence. However, for a more realistic set of functions describing the parameters that compose $R_0(T, \upsilon)$, there is no such a tangent plane as shown in Fig. 12. Therefore, we assumed the following functions:

$$
\begin{aligned}
c(\upsilon) &= c_0\left(1 - e^{-\kappa_1 \upsilon}\right) \\
\alpha_H(\upsilon) &= \alpha_0\left(1 - e^{-\kappa_2 \upsilon}\right) \\
\gamma_H(\upsilon) &= \gamma_0\left(1 + e^{-\kappa_3 \upsilon}\right) \\
a(T) &= a_0\left(1 - e^{-\kappa_4 T}\right) \\
m(T) &= m_0\left(1 - e^{-\kappa_5 T}\right) \\
\mu_M(T) &= \mu_0\left(1 - e^{-\kappa_6 T}\right) \\
\tau(T) &= \tau_0\left(1 - e^{-\kappa_7 T}\right)
\end{aligned}
\tag{61}
$$

with the parameters shown in Table 4, chosen to result in values compatible with the literature [36], we can analyse the relationship between virulence and temperature. This will be done by finding the values of virulence υ that maximizes $R_0(T, \upsilon)$ and then study how this optimal υ changes as temperature changes. First, we calculate

$$
\frac{\partial}{\partial \upsilon} R_0(T, \upsilon) = \frac{\partial c(\upsilon)/\partial \upsilon}{c(\upsilon)} - \left\{ \frac{1}{[\alpha_H(\upsilon) + \gamma_H(\upsilon)]} \times \left[\frac{\partial \alpha(\upsilon)}{\partial \upsilon} + \frac{\partial \gamma(\upsilon)}{\partial \upsilon} \right] \right\} = 0 \tag{62}
$$

and then change the values of temperature to see how those changes affect this maximum fitness. This is done by keeping this maximum fitness fixed, calculated for an initial temperature from Eq. (62), and see what levels of virulence result in this value for each temperature value chosen.

In Fig. 14, we show the result of the numerical simulation of Eq. (50) with the functional shapes of the parameters as in Eq. (61) and numerical values as in Table 4.

Note that $R_0(T, \upsilon)$ reaches a maximum value with variation in virulence and then drops slightly to a stable value. It is also noteworthy that $R_0(T, \upsilon)$ changes more intensely with temperature than with virulence. This is a result of the functional shape and parameter values of the components of $R_0(T, \upsilon)$.

Now, if we change the values of the temperature we can assess what values of virulence keeps that maximum $R_0(T, \upsilon)$ obtained with the initial value of temperature. The result is shown in Fig. 15.

Note that, as $R_0(T, \upsilon)$ is more sensitive to the temperature than to the virulence (see below) an increase in the temperature causes such an in increase in $R_0(T, \upsilon)$ that the parasite can reduce its virulence and still keeps its EES.

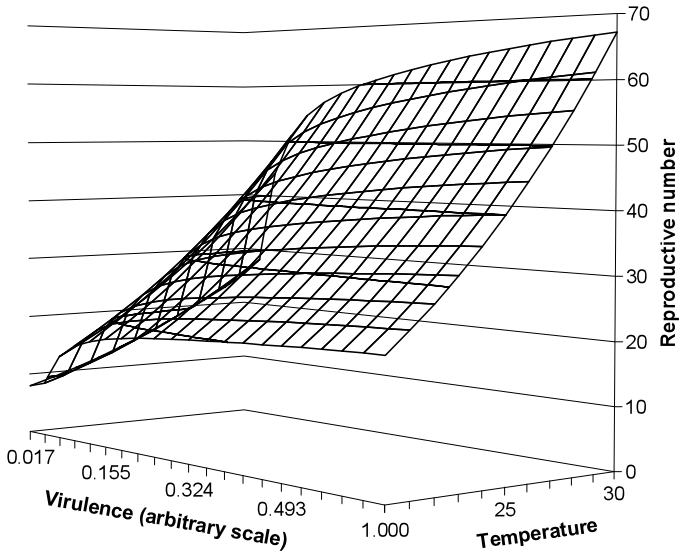

Fig. 14. The basic reproduction number as in Eq. (50) with the functional shapes of the parameters as in Eq. (61) and numerical values as in Table 4.

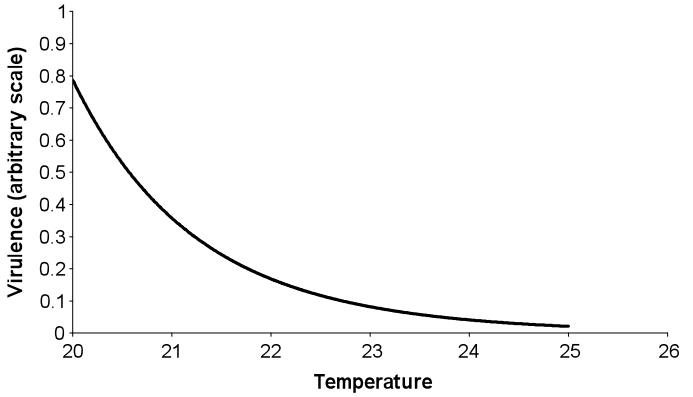

Fig. 15. Effect of the increase in temperature on parasite virulence.

25. Sensitivity of the model to the parameters

In order to estimate the sensitivity of the model to the parameters composing $R_0(T,\upsilon)$ we calculated the partial derivatives of $R_0(T,\upsilon)$ with reference to each one of the factors [18].

We begin by taking the partial derivative of $R_0(T,\upsilon)$ with respect to each of the variables temperature and virulence, that is from Eq. (50) we take first $\frac{\partial R_0(T,\upsilon)}{\partial T}$, which assumes the form:

$$\begin{aligned}\frac{\partial R_0(T,\upsilon)}{\partial T} &= m_0\kappa_5 e^{-\kappa_5 T}\left(a_0\left(1-e^{-\kappa_4 T}\right)\right)^2 + 2m_0\left(1-e^{-\kappa_5 T}\right)a_0\left(1-e^{-\kappa_4 T}\right)a_0\kappa_4 e^{-\kappa_4 T}\\ &\quad\times bc_0\left(1-e^{-\kappa_1\upsilon}\right)\exp\left[-\mu_0\left(1-e^{-\kappa_6 T}\right)\tau_0\left(1-e^{-\kappa_t T}\right)\right]\\ &\quad\times\left\{\mu_0\left(1-e^{-\kappa_6 T}\right)\left[\alpha_0\left(1-e^{-\kappa_2\upsilon}\right)+\gamma_0\left(1+e^{-\kappa_3\upsilon}\right)\right]\right\}\\ &\quad+ m_0\left(1-e^{-\kappa_5 T}\right)\left(a_0\left(1-e^{-\kappa_4 T}\right)\right)^2\\ &\quad\times\left(-bc_0\left(1-e^{-\kappa_1\upsilon}\right)\exp\left[-T^2\tau_0\left(1-e^{-\kappa_7 T}\right)\mu_0\left(1-e^{-\kappa_6 T}\right)\right]\right.\\ &\quad\left.\times T^2\tau_0\left(1-e^{-\kappa_t T}\right)\mu_0\kappa_6 e^{-\kappa_6 T} + T^2\mu_0\left(1-e^{-\kappa_6 T}\right)\tau_0\kappa_7 e^{-\kappa_7 T}\right.\end{aligned}$$

Table 5
Results of the sensitivity analysis.

Parameter	Relative value
$\frac{\partial R_0}{\partial \mu_M}$	1
$\frac{\partial R_0}{\partial \gamma}$	0.038397
$\frac{\partial R_0}{\partial c}$	0.016344
$\frac{\partial R_0}{\partial \alpha_H}$	0.015486
$\frac{\partial R_0}{\partial a}$	0.007479
$\frac{\partial R_0}{\partial m}$	0.000159

$$+ 2T\tau_0\left(1-e^{-\kappa_7 T}\right)\mu_0\left(1-e^{-\kappa_6 T}\right)\times\left[\mu_0\left(1-e^{-\kappa_6 T}\right)\left(\alpha_0\left(1-e^{-\kappa_2 \upsilon}\right)+\gamma_0\left(1+e^{-\kappa_3 \upsilon}\right)\right)\right]^{-1}$$
$$+\frac{bc_0(1-e^{-\kappa_1\upsilon})\exp[-\mu_0(1-e^{-\kappa_6 T})\tau_0(1-e^{-\kappa_t T})]}{T^2\mu_0(1-e^{-\kappa_6 T})(\alpha_0(1-e^{-\kappa_2\upsilon})+\gamma_0(1+e^{-\kappa_3\upsilon}))}$$
$$-\kappa_6\mu_0 e^{-\kappa_6 T}\left[T\left[\mu_0\left(1-e^{-\kappa_6 T}\right)\right]^2\left(\alpha_0\left(1-e^{-\kappa_2\upsilon}\right)+\gamma_0\left(1+e^{-\kappa_3\upsilon}\right)\right)\right]^{-1}\Bigg) \tag{63}$$

Then, we take $\frac{\partial R_0(T,\upsilon)}{\partial \upsilon}$, which results in:

$$\frac{\partial R_0(T,\upsilon)}{\partial \upsilon} = m_0\left(1-e^{-\kappa_5 T}\right)\left[a_0\left(1-e^{-\kappa_4 T}\right)\right]^2\exp\left[-\mu_0\left(1-e^{-\kappa_6 T}\right)\tau_0\left(1-e^{-\kappa_7 T}\right)\right]$$
$$\times c_0\kappa_1 e^{-\kappa_1\upsilon} - m_0\left(1-e^{-\kappa_5 T}\right)\left[a_0\left(1-e^{-\kappa_4 T}\right)\right]^2 b$$
$$\times\exp\left[-\mu_0\left(1-e^{-\kappa_6 T}\right)\tau_0\left(1-e^{-\kappa_7 T}\right)\right]c_0\left(1-e^{-\kappa_1\upsilon}\right)$$
$$\times\mu_0\left(1-e^{-\kappa_6 T}\right)\left[\alpha_0\left(1-e^{-\kappa_2\upsilon}\right)+\gamma_0\left(1+e^{-\kappa_3\upsilon}\right)+\upsilon\kappa_2 e^{-\upsilon\kappa_2}-\upsilon\kappa_3\gamma_0 e^{-\kappa_3\upsilon}\right] \tag{64}$$

Applying the same numerical values as those used to construct Fig. 14 in Eqs. (63) and (64) we conclude that the model is more than 40 times more sensitive to temperature than to virulence.

In terms of the functional forms chosen for the parameters (with the exception of b that was considered as constant through all the calculations) this results in:

$$\frac{\partial R_0}{\partial a} = \frac{2ambc\exp(-\mu_M\tau)}{\mu_M(\alpha_H+\gamma_H)} \tag{65}$$
$$\frac{\partial R_0}{\partial m} = \frac{a^2bc\exp(-\mu_M\tau)}{\mu_M(\alpha_H+\gamma_H)} \tag{66}$$
$$\frac{\partial R_0}{\partial c} = \frac{a^2mb\exp(-\mu_M\tau)}{\mu_M(\alpha_H+\gamma_H)} \tag{67}$$
$$\frac{\partial R_0}{\partial \alpha_H} = -\frac{\alpha a^2mbc\exp(-\mu_M\tau)}{(\mu_M(\alpha_H+\gamma_H))^2} \tag{68}$$
$$\frac{\partial R_0}{\partial \gamma_H} = -\frac{\gamma a^2mbc\exp(-\mu_M\tau)}{(\mu_M(\alpha_H+\gamma_H))^2} \tag{69}$$
$$\frac{\partial R_0}{\partial \mu_M} = \frac{a^2mbc}{(\alpha_H+\gamma_H)}\left[-\frac{1}{\mu_M^2}\exp(-\mu_M\tau)-\frac{1}{\mu_M}\exp(-\mu_M\tau)\right] \tag{70}$$

which in terms of the functions as in Eqs. (59) and Table 4 result in the relative sensitivity scale as in Table 5.

Therefore, with the forms chosen for the parameters, the model is more sensitive to variations in the mosquitoes' mortality rate than to the other parameters.

The results shown in Figs. 13 and 15 are obviously incompatible and this deserves an explanations. In the simplest case a tangent plane, as shown in Fig. 12, was assumed to describe the maximization of $R_0(T,\upsilon)$ with temperature and virulence. As the parameters describing such a situation were not know we simply assumed them all as equal to

one. However, the functions describing the components of $R_0(T, \upsilon)$ as in Eq. (59) rarely (if at all) result in a tangent plane. Therefore, we believe that this simplest case has only theoretical value and only exceptionally expresses any real situation. Therefore, the so-called more realistic case is probably the likely to describe what happens in nature.

Although our results are obviously strongly dependent on the form chosen for the temperature and virulence dependence of the parameters of R_0, expressed in the relations (10), we believe that we have demonstrated that for the set of conditions applied a clear increase trend in virulence is observed with the increase in temperature. Other relationships between the parameters and the temperature and virulence could produce different outcomes from the model. However, we think that the forms chosen are reasonable in the sense that they reproduce what should be expected to happen for subtle variations in both temperature and virulence.

The most strongly evidence-based relationship is the one between the size of the mosquito population and temperature. This was based on the observation that higher temperature and the absence of drying result in an increased production of adult mosquitoes [73,74]. The mosquito's longevity, in contrast, decreases with temperature [75], which justifies the relationship chosen for mosquito mortality rate μ and temperature.

26. Final comments

The impact of global warming on the spread of insect-borne infections is likely to be highest in the areas most affect by the increase in the average temperature. So, the northern hemisphere, known to be more affected by global warming than the southern hemisphere [76,77] is likely to have a highest number of new vector-borne infections than the tropical world. As a matter of fact, in recent years there have been several cases of vector-borne diseases reported in the northern hemisphere, like dengue in France [78], leishmaniasis in France [79], chikungunya in Italy [80], and West Nile Virus in the United States [81]. In the tropical world, it is expected a worsening of existing vector-born infections. However, several reports are pointing to an odd reduction in some insect-transmitted infections, like malaria [82,83], perhaps due to the impact of public-health measures such as improved medications, widespread insecticide use and bed nets. Nevertheless, it is almost certain that these public-health measures implemented to reduce the incidence of malaria will tend to be much more expensive in a context of increased temperature, rainfall and human migration expected to result from climate change.

Increased spread of insect-borne diseases is likely in a warmer world. Tools to deal with such scenario, like the models here reviewed, can be extremely helpful in planning measures to mitigate its effects.

References

[1] Bloom AJ. Global climate change. Sunderlad, Massachusetts: Sinauer Associates Inc. Publishers; 2010.
[2] Houghton JT, Jenkins GJ, Ephraums JJ. Climate change. The IPCC assessment. Cambridge: Cambridge University Press; 1990.
[3] Costello A, Abbas M, Allen A, Ball S, Bell S, Bellamy R, et al. Managing the health effects of climate change. The Lancet 2009;373:1693–733.
[4] McMichael AJ. Planetary overload. Global environment change and the health of the human species. Cambridge: Cambridge University Press; 1993.
[5] WHO. Potential health effects of climate change: Report of a WHO Task Group (WHO/PEP/90/10). Geneva: WHO; 1990.
[6] Haines A, Fuchs C. Potential impact on health of atmospheric change. Journal of Public Health Medicine 1991;13:69–80.
[7] International Federation of Red Cross and Red Crescent Societies. World Disaster Report 2004. IFRC; 2004 [Ch. 2].
[8] Kosatsky T. The 2003 European heat waves. Euro Surveillance. Published online July 2005, 10(7). http://eurosurveillance.org/en/v10n07/1007-222.asp.
[9] Luterbacher J, Dietrich D, Xoplaki E, Grosjean M, Wanner H. European seasonal and annual temperature variability, trends, and extremes since 1500. Science 2004;303:1499–503.
[10] Patz JA, Campbell-Lendrum D, Holloway T, Foley JA. Impact of regional climate change on human health. Nature 2005;438:310–7.
[11] Massad E, Forattini OP. Modelling the temperature sensitivity of some physiological parameters of epidemiologic significance. Ecosystem Health 1998;4(2):119–29.
[12] Ralisoa O. *Plasmodium falciparum* malaria transmission indices in a highland village in the Ikopa River valley near Antananarivo. Madagascar Parasitologia 1992;33:219–23.
[13] Gill CA. The role of meteorology in malaria. Indian Journal of Medical Research 1921;8:633–93.
[14] Hay SI. Remotely sensed surrogates of meteorological data for the study of the distribution and abundance of arthropod vectors of disease. Annals of Tropical Medicine and Parasitology 1996;90:1–19.
[15] Khasnis AA, Nettlelman MD. Global warming and infectious disease. Archives of Medical Research 2005;36:689–96.
[16] Sutherst RW. Global change and human vulnerability to vector-borne diseases. Clinical Microbiology Reviews 2004;17(1):136–73.
[17] Lopez LF, Coutinho FAB, Burattini MN, Massad E. Threshold conditions for infection persistence in complex host–vectors interactions. Comptes Rendus Biologies Académie des Sciences Paris 2002;325:1073–84.

[18] Macdonald G. The analysis of equilibrium in malaria. Tropical Disease Bulletin 1952;49:813–28.
[19] Dietz K. The estimation of the basic reproduction number for infectious diseases. Statistical Methods in Medical Research 1993;2:23–41.
[20] Burattini MN, Coutinho FAB, Lopez LF, Massad E. Modelling the dynamics of leishmaniasis considering human, animal host and vector populations. Journal of Biological Systems 1998;6(4):337–56.
[21] Diekmann O, Heesterbeek JP, Metz JAJ. On the definition and the computation of the basic reproduction ratio R_0 in models for infectious diseases in heterogeneous populations. Journal of Mathematical Biology 1990;28:365–82.
[22] Diekmann O, Heesterbeek JP. Mathematical epidemiology of infectious diseases. Chichester: John Wiley & Son Ltd; 2000.
[23] Garret-Jones C. Prognosis for the interruption of malaria transmission through assessment of the mosquito's vectorial capacity. Nature 1964;204:1173–5.
[24] Anderson RM, May RM. Infectious diseases of humans: dynamics and control. Oxford, New York: Oxford University Press; 1991 [752 pp.].
[25] Molineaux L, Gramiccia G. The Garki project. Geneva: World Health Organization; 1980 [311 pp.].
[26] Coutinho FAB, Burattini MN, Lopez LF, Massad E. Threshold conditions for a non-autonomous epidemic system describing the population dynamics of dengue. Bulletin of Mathematical Biology 2006;68:2263–82.
[27] Floore T. Mosquito information. The American Mosquito Control Association. http://www.mosquito.org/info.php, July 1, 2004.
[28] Beaty BJ, Marquardt WC. The biology of disease vectors. Niwot: University Press of Colorado; 1996.
[29] Hauck Center for the Albert B. Sabin Archives, Box 12, file 5. http://sabin.uc.edu/dengue.ucm, 2005.
[30] El'sgol'ts EL. Introduction to the theory of differential equations with deviating arguments. San Francisco: Holden-Day Inc.; 1966.
[31] Rodahin F, Rosen L. Mosquito vectors and dengue virus-vector relationships. In: Gubler DJ, Kuno G, editors. Dengue and dengue hemorrhagic fever. New York: CABI Publishing; 1997.
[32] Forattini OP. Medical culicidology. São Paulo: EDUSP; 2002 [in Portuguese].
[33] Shroyer DA. Vertical maintenance of dengue-1 virus in sequential generations of *Aedes albopictus*. J Am Mosq Control Assoc 1990;6(2):312–4.
[34] Joshi V, Mourya DT, Sharma RC. Persistence of dengue-3 virus through transovarial transmission passage in successive generation of *Aedes aegypti* mosquitoes. Am J Trop Med Hyg 2002;67(2):158–61.
[35] Crochu S, Cook S, Attoui H, Charrel RN, Chesse RD, Belhouchet M, et al. J Gen Virol 2004;85:1971–80.
[36] Burattini MN, Chen M, Chow A, Coutinho FAB, Goh KT, Lopez LF, et al. Modelling the control strategies against dengue in Singapore. Epidemiol Infect 2008;136(3):309–19.
[37] National Environmental Agency, Ministry of Environment and Water Resources of Singapore. NEA's key operation strategies in dengue control. September 2005.
[38] Coutinho FAB, Burattini MN, Lopez LF, Massad E. An approximate threshold condition for non-autonomous system: An application to a vector-borne infection. Math Comp Simul 2005;70:149–58.
[39] Massad E, Forattini OP. Modelling the temperature sensitivity of some physiological parameters of epidemiological significance. Ecosystem Health 1998;4(2):119–29.
[40] Dobson A. Biodiversity. Lancet 1993;342:1096–9.
[41] Bates M. The natural history of mosquitoes. New York: MacMillan Company; 1949.
[42] Prochnow O. Die Temperaturkurve der Entwicklungsgeshwidigkeit für Pflazen und poikilothermen Tiere. Entomologische Zeitschrift 1907;20:313–4.
[43] Prochnow O. Die Abhängigkeit der Entwicklungs und Reaktionsgehwidigkeit bei Pflanzen un poikilothermen Tiere von der Temperatur. Inaugural-Dissertationen Berlin Universität, 1908 [350 pp.].
[44] Bates M. The development and longevity of Haemagogus mosquitoes. Annals Entomological Society of America 1947;40:1–12.
[45] Dye C. The analysis of parasite transmission by bloodsucking insects. Annual Review of Entomology 1992;37:1–19.
[46] Carpenter SJ, La Casse WJ. Mosquitoes of North America. Berkley: University of California Press; 1955 [360 pp.].
[47] Mayne B. Notes on the influence of temperature and humidity on oviposition and early life of *Anopheles*. Reports of US Public Health 1926;41:986–90.
[48] Bishop FC. Notes on certain points of economic importance in the biology of the house-fly. Journal of Ecological Entomology 1915;8:54–71.
[49] Schubert W. Biologische Untersuchungen über die Rüberblattwanze, Pesma quadrata, Fieb., im schelchen Befallgebiet. Zeitschrift fuer Angewandte Entomologie 1928;13:129–55.
[50] Rose MR, Charleworth B. A test of evolutionary theories of senescence. Nature 1980;287:141–2.
[51] Thomson RCM. Studies on the behaviour of *Anopheles minimus*, Pt. III: The influence of water temperature on the choice and suitability of the breeding place. Journal of the Malaria Institute of India 1940;3:323–48.
[52] Russel PF, Rao TR. Observation on longevity of *Anopheles culicifacies* imagines. American Journal of Tropical Medicine 1942;22:517–33.
[53] Stratman-Thomas WK. The influence of temperature on *Plasmodium vivax*. American Journal of Tropical Medicine 1940;20:703–15.
[54] Burattini MN, Coutinho FAB, Massad E. Malaria transmission rates estimated from serological data. Epidemiology and Infection 1993;111:503–23.
[55] Anderson RM, May RM. The population dynamics of microparasites and their invertebrate hosts. Phil Trans R Soc Lond B, Biol Sci 1981;291:451–524.
[56] Massad E. Transmission rates and the evolution of pathogenicity. Evolution 1987;41(5):1127–30.
[57] Ewald EW. The evolution of infectious diseases. Oxford: Oxford University Press; 1994.
[58] Levin BR. The evolution and maintenance of virulence in microparasites. Emerg Infect Dis 1996;2:93–192.
[59] Day T. Parasite transmission modes and the evolution of virulence. Evolution 2001;55(12):2389–400.
[60] Day T. On the evolution of virulence and the relationship between various measures of mortality. Proc R Soc Lond B 2002;269:1317–23.
[61] Day T. The evolution of virulence in vector-borne and directly transmitted parasites. Theor Pop Biol 2002;62:199–213.

[62] Lively CM. The ecology of virulence. Ecol Lett 2006;9:1089–95.
[63] Day T, Graham AL, Read AF. Evolution of parasite virulence when host responses cause disease. Proc R Soc Lond B 2007;274:2685–92.
[64] Levin BR, Pimentel D. Selection of intermediate rates of increase in parasite-host systems. Am Nat 1981;117:308–15.
[65] May RM, Anderson RM. Epidemiology and genetics in the co-evolution of parasites and hosts. Proc R Soc Lond B 1983;219:281–313.
[66] Bremermann HJ, Pickering J. A game-theoretical model of parasite virulence. J Theor Biol 1983;100:411–26.
[67] Frank SA. Models of parasite virulence. Q Rev Biol 1996;71:37–78.
[68] Sutherst RW. Implications of global change and climate variability for vector-borne diseases: generic approaches to impact assessments. Int J Parasitol 1998;28:935–45.
[69] Forattini OP, Kakitani I, Massad E, Marucci D. Studies on mosquitoes (Diptera: Culicidae) and anthropic environment. 3. Survey of adult stages at the rice irrigation system and the emergence of Anopheles albitarsis in South-Eastern Brazil. Revista de Saúde Pública 1993;27(5):313–25.
[70] Forattini OP, Kakitani I, Massad E, Marucci D. Studies mosquitoes (Diptera: Culicidae) and anthropic environment. 9. Synanthropic and epidemiological vector role of Aedes scapularis in South-Eastern Brazil. Revista de Saúde Pública 1995;29(3):199–207.
[71] Koella JC, Turner P. Evolution of parasites. In: Stearns SC, Koella LC, editors. Evolution in health and disease. Oxford: Oxford University Press; 2008. p. 229–38 [Ch. 17].
[72] Dieckmann U. Adaptive dynamics of pathoge-host interactions. In: Dieckmann U, Metz JAJ, Sabelis MW, Sigmund K, editors. Adaptive dynamics of infectious diseases. Cambridge University Press; 2002. p. 39–59.
[73] Massad E, Forattini OP. Modelling the temperature sensitivity of some physiological parameters of epidemiologic significance. Ecosystem Health 1998;4(2):119–29.
[74] Alto BW, Juliano SA. Precipitation and temperature effects on population of *Aedes albopictus* (Diptera: Culicidae): implications for range expansion. J Med Entomol 2001;38(5):646–56.
[75] Hawley WA. The effect of larval density on adult longevity of a mosquito, *Aedes sierrenses*: epidemiological consequences. J Anim Ecol 1985;54:955–64.
[76] Moberg A, Sonechkin DM, Holmgren K, Datsenko NM, Karlén W. Highly variable Northern hemipshere temperatures reconstructed from low- and high-resolution proxy data. Nature 2005;433:613–7.
[77] Hoghton J. Global warming. Reports on Progress in Physics 2005;68:1343–403.
[78] http://www.france24.com/en/20100913-mosquito-borne-dengue-fever-arrives-france-dirst-case-nice-health. Accessed 27 September 2010.
[79] Buffet PA, Morizot G. Cutaneous leishmaniasis in France: towards the end of injectable therapy? Bulletin de la Societé du Pathologie Exotic 2003;96(5):383–9.
[80] Beltrame A, Angheben A, Bisoffi Z, Monteiro G, Marocco S, Calleri G, et al. Imported chikungunya infection, Italy. Emerging Infectious Diseases 2007;13(8):1264–6.
[81] Hun GD, Sejvar J, Montgomery SP, Dworkin MS. West Nile Virus in the United States: an update on an emerging infectious disease. American Family Physicians 2003;68(4):653–61.
[82] Gething PW, Smith DL, Patil AP, Tatem AJ, Snow RW, Hay SI. Climate change and the global malaria recession. Nature 2010;465:342–6.
[83] Behrens RH, Carrol B, Smith V, Alexander N. Declining incidence of malaria imported into the UK from West Africa. Malaria Journal 2008;7:235. doi:10.1186/1475-2875-7-235.